SCIENTIFIC COMMITTEE

NINETEENTH REGULAR SESSION

Koror, Palau

16-24 August 2023

Review and analyses to inform conceptual models of population structure and spatial stratification of bigeye and yellowfin tuna assessments in the Western and Central Pacific Ocean

WCPFC-SC19-2023/SA-WP-02

26 July 2023

Paul Hamer[1], Jed Macdonald[1], Joanne Potts[1], Tiffany Vidal[2], Thom Teears[1], Inna Senina[1]

[1]Oceanic Fisheries Programme (OFP), Pacific Community (SPC), Noumea, New Caledonia

[2]South Pacific Regional Fisheries Management Organisation

Executive summary

This paper was developed in response to a recommendation from the peer review of the 2020 yellowfin tuna assessment (Punt et al., 2023) for better information to understand the basis for spatial structure of the WCPO yellowfin tuna assessment, and to explore whether simplified spatial structures are supported by such information and conceptual population models. The peer review also recommended using analysis of size composition data as part of this exploration, as has occurred for assessments conducted by the Inter-American Tropical Tuna Commission (IATTC). This paper considers both yellowfin and bigeye tuna as these assessments have been conducted using the same spatial and fishery structures and the peer review questioned whether different structures might be more appropriate.

The paper reviews previous model spatial structures, and a range of biological information, tagging data, fishery CPUE data and predictions of SEAPODYM models to develop conceptual models of population structuring in yellowfin and bigeye stocks across the Pacific, with a focus on the WCPO assessment region. To build on the review information, two additional analyses of fishery dependant data were conducted. Firstly, a statistical analysis (regression trees) of spatial patterns in length and weight compositions for longline fishery catches in the WCPO. Secondly, an analysis of spatial coherence and predictability of longline CPUE time series across the Pacific using Convergent Cross Mapping within an Empirical Dynamic Modelling framework. The results were considered in an overall synopsis that provides suggested alternative spatial stratifications to be explored for the yellowfin and bigeye assessments in the WCPO.

Overall, the results support options for simpler model stratifications with slight differences between the species. However, the simplest models that might be considered suitable based on the review and analysis conducted will likely require added complexity to accommodate wider modelling requirements including the incorporation of tag data and the associated assumptions (i.e., tag mixing periods). Ultimately the information presented is also consistent with the current 9 region model and this may continue to be applied for both stocks. However, it is possible that models based on simpler spatial structures may perform better, run faster and improve the efficiency of assessments. Exploration of the suggested simpler model structures is required. Changing model spatial structures has flow on implications for other work including management strategy evaluation modelling and bio-economic evaluations, thus we suggest it is probably better to be considered carefully as a separate modelling research exercise outside of the standard stock assessment work and reported to SC for their consideration prior to the next yellowfin and bigeye assessments.

We invite the SC19:

- To consider the information in this paper and its implications for bigeye and yellowfin stock assessment spatial structure.
- Note that while simpler model structures are supported by the review, the information does not suggest that application of the current 9 region model is inappropriate.
- Consider whether to support a separate study to explore models of alternative spatial structure to better understand if simpler model structures might provide more optimal model performance and efficiency of stock assessments, and implications for other uses of the assessment models and outputs.

Contents

Background

Spatial structure of stock assessment models can impact strongly on model estimated quantities, and hence fishery management outcomes (Cadrin, 2020; Cadrin et al., 2023; Hilborn, 2003). A key premise for incorporating explicit spatial structure or 'strata' into a stock assessment is that there is some identifiable or underlying spatial heterogeneity in the processes that influence the dynamics of populations, including the impacts of fishing, within a broader stock region (Cadrin et al., 2023; Goethel et al., 2023). Defining spatial strata in tropical tuna assessments is particularly challenging given their migratory nature and the large geographic scale over which tuna stocks are dispersed and that stock assessments must cover. Furthermore, there is often limited knowledge on the spatial heterogeneity of biology and ecological processes that influence local/regional population dynamics. To complicate things even more, subpopulation structures and/or biological heterogeneities may not be consistent over time due to the changing dynamics of oceanographic features that influence tuna dispersal, habitat suitability and feeding conditions. Notable of these in the Pacific is the El Nino Southern Oscillation and its influence on east-west spatial dynamics of tropical tunas in the equatorial region (Nicol et al., 2022).

The independent peer review of the 2020 stock assessment of yellowfin tuna in the western and central Pacific Ocean (WCPO) (Punt et al., 2023) recognised that the 9 region spatial stratification used in that assessment (and the two previous assessments) presented difficulties for stable model estimation of key process such as recruitment and movement, among other concerns. The peer review indicated that the model spatial stratification was likely too complex and should be reviewed. It was also recommended that this review be based on developing a conceptual model of the spatial structure of yellowfin populations in the WCPO and the fisheries catching them. The peer review also questioned the justification for applying the same spatial stratification for the WCPO yellowfin and bigeye assessments, recommending that spatial stratification be considered independently for these assessments.

Most current age structured stock assessment frameworks (including MULTIFAN-CL) cannot incorporate spatially varying processes such as growth and natural mortality. However, with the assumption that these processes are spatially consistent, population dynamics can be estimated for spatial strata within a broader modelled stock by estimating spatially explicit parameters such as recruitment, total mortality and movement among strata to explain spatially stratified observations (i.e., fisheries catch and size composition, tag-recaptures and CPUE indices). Defining spatial strata in a stock assessment can help to better explain patterns in the data such as fishery size composition and CPUE indices of abundance, and potentially to provide spatially explicit management advice, such as local depletion levels. Achieving the possible benefits of spatial stratification has a cost in terms of increased data needs and model parametrisation (i.e., tagging data to inform on movement among model strata, abundance indices for each model strata, sufficient size or age composition data at finer spatial scales etc.), and this may often be the limiting factor for incorporating spatial structure into an assessment, even when other information suggest population structure exists.

For widely dispersed highly migratory species such a yellowfin and bigeye tuna that span 1000's of kilometres latitudinally and longitudinal across both hemispheres of the Pacific, through many EEZs and high seas, and between the jurisdictions of Regional Fisheries Management Organisations (RFMOs), there is a strong desire to provide spatially explicit management advice informed by spatially explicit stock assessments. Introducing spatial stratification into an assessment should however be underpinned by a 'conceptual model' of the stock being assessed that aims to identify spatial heterogeneities in both biology and fishery characteristics. As stated by Cadrin et al., (2023) *best scientific practices for defining spatial boundaries, spatial structure, and fleet structure in stock assessment should consider biological reality, theoretical assumptions, and practical solutions for meeting fishery management objectives.* Ultimately any spatially stratified assessment will need to consider all these factors, and in the light of the available data.

This paper responds to a recommendation from the peer review of the 2020 yellowfin stock assessment to provide a conceptual basis for spatial structure of the stock assessments for yellowfin and bigeye tuna in the WCPO. It describes work done to inform conceptual models of spatial population and fishery structure to inform consideration on appropriate, and potentially simplified, spatial stratification for yellowfin and bigeye tuna assessments in the WCPO. The paper recommends alternative spatial stratifications that could be explored in the 2023 assessments, and comments on the suitability of the current 9 region spatial structure.

Revisiting spatial stratification in 2023

Spatial stratification of stock assessment models may need to be adjusted to accommodate new knowledge, new data, improved approaches for modelling certain data (i.e., tag data) and better appreciation of the information in the data to inform processes such a movement in a spatially explicit model. This review aims to consider information on biology, phenotypic and genotypic variation, tagging data, patterns in fishery dependent size compositions and CPUE time series and predictions from integrated bio-physical models (SEAPODYM) (Lehodey et al., 2008) to provide a basis for informing spatial stratification of yellowfin and bigeye tuna assessments in the WCPO.

Review of previous spatial structures

Stock assessments of yellowfin and bigeye tuna in the WCPO have been spatially structured since they were first conducted. The changes in spatial stratification are shown in Figure 1. The first yellowfin assessment in the WCPO by Hampton and Fournier (2001) applied a 7 region model stratification that was based on the distribution of the various fisheries defined in the model and the spatial resolution of some of the data (Figure 1a). The yellowfin, and bigeye, WCPO assessments were next conducted in 2003 (Hampton et al., 2003; Hampton and Kleiber, 2003) and 2004 (Hampton et al., 2004a, 2004b). These assessments applied a consistent 5 region stratification that was justified to separate out the tropical area where both surface and longline fisheries occur (Figure 1b).

In 2005 the bigeye and yellowfin assessments were again conducted (Hampton et al., 2005a; Hampton et al., 2005b) but this time with a 6 region model stratification (Figure 1c). The rationale for this stratification was slightly nuanced from the 5 region model, *to separate the tropical area, where both surface and longline fisheries occur year-round, from the higher latitudes, where the longline fisheries occur more seasonally and in response to discussions held at SCTB 17 on the previous stratification.* From this point on the 6 region model stratification was applied for bigeye and yellowfin assessments through to 2011, although a 7 region stratification (additional region for the Indonesia/Philippines/Vietnam area) (Figure 1d) was run as a sensitivity in the 2006 assessments (Hampton et al., 2006a, 2006b). Comparison of the WCPO with a Pacific-wide assessment for bigeye was also conducted around that time (Hampton and Maunder, 2006, 2005), and employed an 8 region model stratification, that retained the 6 region WCPO stratification.

In 2012, the 2011 bigeye assessment underwent an independent peer review (Ianelli et al., 2012), where the 6 region stratification was reviewed. In this review it was noted that the 6 region stratification was defined such that:

I. broad “ecological” regions are reflected;

II. there are sufficient fisheries data in each region to enable estimation of important region-specific parameters;
III. the regions reflect fishery characteristics, particularly homogeneity of CPUE and size composition as far as possible; and
IV. for management analyses using the assessments, it is necessary to have the same (or at least comparable) spatial configuration for the three tropical tuna species, skipjack, yellowfin and bigeye.

Although not explicitly mentioned it has also been recognised that maintaining consistent spatial strata for yellowfin and bigeye is desirable for efficiency in preparing data inputs, CPUE analysis and running models, noting that these two assessments are typically run in parallel under the WCPFC assessment scheduling.

The 2011 bigeye peer review, while not discounting the 6 region stratification, was concerned about tag mixing assumptions and the influence of high recapture rates in one small area of region 5 off eastern Australia that related to several targeted tagging cruises in the Coral Sea (see Figure 3). This tagging occurred on regular aggregations of sub-adult and adult yellowfin and bigeye that occur in this area. Removing those tag data from the model would remove potentially valuable information on movement and possibly natural mortality. To mitigate these issues the analysts at the time implemented several smaller model regions to encompass localised areas where lots of tags were released and recaptured (i.e., region 9) and/or movements and broader mixing of tagged fish were known to be less extensive (i.e., region 8, Papua New Guinea/Solomons) (Figure 1e), with the idea that tag mixing assumptions and implications of high localised recapture rates could be better dealt with by including these smaller regions. They also recognised that the large difference in the fisheries (i.e., gears/selectivities/data quantity and quality) in the region around the Indonesia/Philippines/Vietnam warranted a separate region (i.e., region 7) (Figure 1e), and that this was possible with improvements in data available for that region. This culminated in the first 9 region spatial stratification being implemented in the 2014 yellowfin and bigeye assessments (Davies et al., 2014; Harley et al., 2014) (Figure 1e).

The Pacific-wide bigeye assessment was again explored in 2015, this time using a 12 region stratification (McKechnie et al., 2015), that retained the new 9 region stratification for the WCPO. The 2015 Pacific-wide bigeye assessment concluded that the dynamics of bigeye tuna in the WCPO estimated using the Pacific-wide model were not substantially different from those estimated using the WCPO-only model, especially with respect to the main stock status indicators used by WCPFC. The authors suggested that it was reasonable to continue to provide management recommendations to WCPFC on the basis of WCPO region stock assessment models. They further acknowledged that a significant potential misspecification of the Pacific-wide model was the assumption of common growth across the Pacific when actual growth rates and maximum size and size at maturity of bigeye are known to vary between the western and eastern Pacific. None-the-less there is no clear separation between the eastern and western Pacific bigeye populations (discussed in later sections) and interest in Pacific-wide bigeye assessments continues, with recent work being led by the IATTC.

The 9 region stratification continued for the 2017 assessments (McKechnie et al., 2017; Tremblay-Boyer et al., 2017) and was modified slightly in the 2020 assessments by moving the northern boundaries of regions 3 and 4 from 20°N to 10°N (Ducharme-Barth et al., 2020; Vincent et al., 2020) to better isolate the tropical region surface and longline fisheries (Figure 1f).

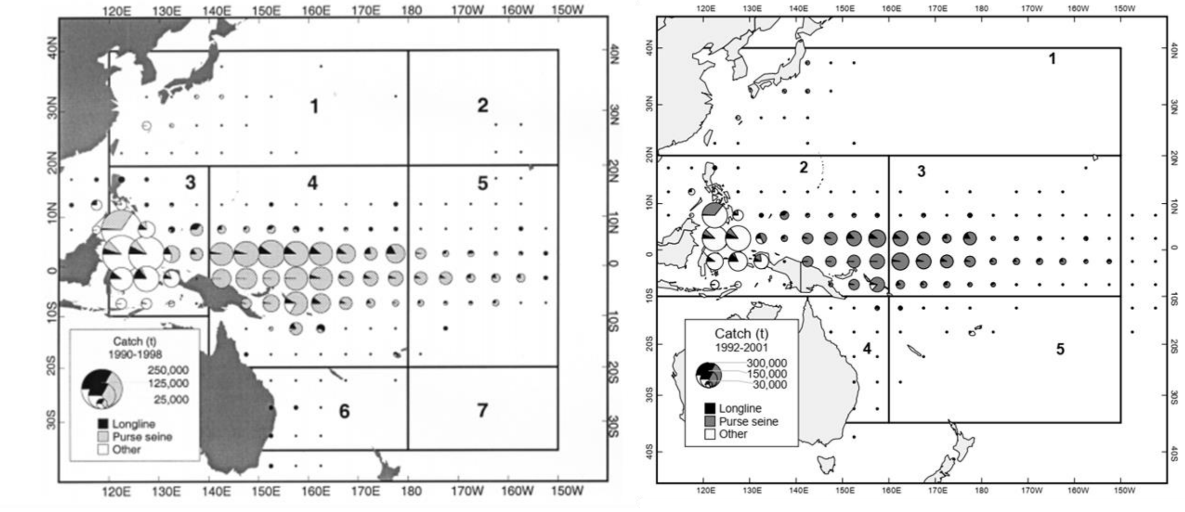
a) 2001, yellowfin, 7 region

b) 2003 and 2004, yellowfin and bigeye, 5 region

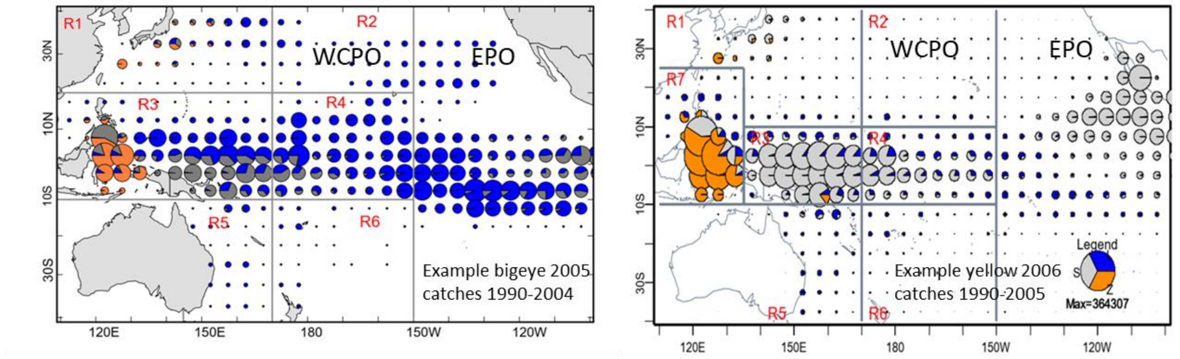
c) 2005-2011, yellowfin and bigeye, 6 region

d) 2006, yellowfin and bigeye, 7 region sensitivity

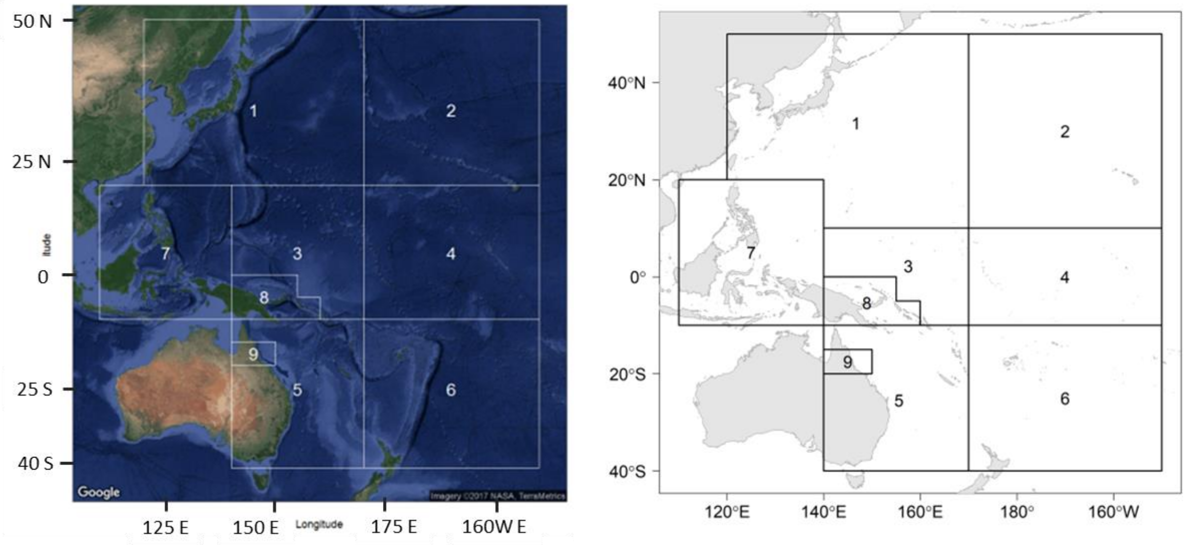
e) 2014, 2017, yellowfin and bigeye, 9 region

f) 2020, yellowfin and bigeye, 9 region

Figure 1 Evolution of spatial stratification of yellowfin and bigeye stock assessments in the WCPO.

Methods

Biological information

This review component covers biology, including reproductive biology, spawning areas, age and growth; genetic and non-genetic studies, tagging data, otolith chemistry, morphometrics and parasites. There are substantial tagging data for both bigeye and yellowfin tuna, involving traditional and archival tags that are also considered. It draws on the information and literature summarised in the extensive review by Moore et al., (2020).

In addition to this review, recent work has analysed the historic data sets on larval tuna distribution, mostly collected by the Japanese research cruises from the 1950's to early 1980's and originally reported in Nishikawa et al., (1985). Recent papers have presented digitised versions of larval tuna data distributions in global oceans (Buenafe et al., 2022; Reglero et al., 2014) and the Nishikawa et al., (1985) data have been digitised and analysed using geospatial statistical models for the Pacific Ocean by Ijima and Jusup (2023). Studies on larval tuna distribution and abundance have also recently been published for the Philippines region (Nepomuceno et al., 2020). These studies provide indications of spawning and larval rearing/dispersal areas for bigeye and yellowfin, as well as other tuna.

The biological information review attempts to identify evidence for population structure based on defined spawning areas, variation in vital rates such as growth, genetic and or phenotypic heterogeneity, and tag-recapture patterns. Other information that is also considered included spatial patterns in CPUE levels for the longline fishery from the Pacific wide CPUE analysis by Ducharme-Barth et al., (2020). This is a qualitative review exercise and results are included in Appendix 1 along with the related citations and summarised below. Conceptual diagrams are developed to try to capture the major features of population structure that would be relevant to considering the stratification of stock assessments.

Information from SEAPODYM

SEAPODYM (Spatial Ecosystem And POpulation DYnamics Model) (Lehodey et al., 2008; Senina et al., 2008; Senina et al., 2020) is a numerical model based on an underlying advection-diffusion-reaction equation with age structure. SEAPODYM simulates the change in abundance of a fish species population over time, 2D space and age. In addition, the model considers the life stages, from the larval to the mature adult stage, distinguished by different movement dynamics. To model physical-biological interactions between fish populations and the ocean pelagic ecosystem, SEAPODYM has a small number of parameters linking rates of reproduction, mortality, and movement with environmental variables. Quantitative methods, including global sensitivity analysis, a maximum likelihood estimation (MLE) approach, uncertainty analysis and statistical validation, are used to estimate model parameters and to provide model estimates that are consistent with observations.

In this review the outputs produced by SEAPODYM models for yellowfin (Nicol et al., 2022; Senina et al., 2015; Senina et al., 2023) and bigeye tuna (Hampton et al., 2023; Lehodey et al., 2010; Senina et al., 2021; Senina et al., 2023) in the Pacific are interpreted in relation to spatial stratification of the stock assessments. The latest version of the SEAPODYM models for bigeye and yellowfin were used to generate spatial maps of the predicted abundance of larvae, juvenile, and adults throughout the Pacific Ocean (Senina et al., 2023).

Analysis of fishery size composition

In this analysis we use length-frequency (LF) and weight-frequency (WF) data for bigeye and yellowfin tuna caught via longline (LL) at a 5° x 5° spatial resolution across the Western and Central Pacific Ocean (WCPO) since 1990. During exploratory analyses, length composition data from purse seine unassociated (PSU) and associated (PSA) sets were found to be spatially and temporally sparse throughout the full WCPO and were very much focussed on the tropical equatorial region. While these data were analysed, they did not appear to have clear spatial heterogeneity (very low variance explained) and because assessment regions are required for the entire WCPO region we focus only on the results for the longline (LL) analysis in this paper.

The aim of this analysis was to use a statistical method to aggregate these data into contiguous regions that have similar catch size compositions. Spatial groupings derived from the analyses can be informative of spatial differences in processes that influence the size compositions. These processes could be either biological or related to differences in selectivity/catchability. They may also be influenced by variation in the way size compositions are sampled (i.e., spatial sampling biases), and this should also be considered when interpreting results of this type of multi-fleet data. Assuming that sampling biases are not substantial, spatial groupings of similar size compositions can indicate heterogeneity that should be considered with respect to spatial stratification of the stock assessments, either in respect of fishery groupings or underlying population processes (Lennert-Cody et al., 2010).

LF and WF data for each species were analysed separately following methods of Lennert-Cody et al., (2010) and Lennert-Cody et al., (2013). That is, a regression tree algorithm was implemented using the FishFreqTree package (v. 3.3.2) (Xu and Lennart-Cody, 2023) in R (v. 4.3.0, R Core Team, 2023) that continuously splits LF or WF data into homogenous subgroups. This is done sequentially, whereby data are split at a single location that provides the greatest decrease in heterogeneity/impurity within each subgroup.

Data were pooled across the time period from 1990 to 2020, and if there were fewer than 50 length or weight observations within a 5° x 5° grid cell, this grid cell was excluded from the analysis. We explored analyses of subsets of the data for historical (pre-2010) and recent time periods (post-2010), but the results were similar to the full data set, so we only include the full data set analyses here. Split location was only based on latitude or longitude, year was excluded from split choice to ensure resulting zones (i.e., spatial groupings) were spatially continuous and did not have 'holes' (see Discussion). The number of requisite splits was explored based on (1) percentage variance explained (%var) by accumulative splits, and (2) interrogation of the LF and WF histograms within each defined zone. If the histograms within each defined zone exhibited bimodality or 'shoulders' in their distributions, it would be indicative of unmodelled heterogeneity and suggest that further splits were required.

Analysis of Pacific wide longline CPUE time series

In this analysis we explore a novel approach to identify geographically distinct signals in fishery-dependent catch per unit effort data (CPUE). Using a 69-year (1950-2018 inclusive) times series of CPUE for yellowfin and bigeye tuna from the commercial longline fishery operating throughout the Pacific Ocean basin, we develop an approach using convergent cross mapping (CCM) (Sugihara et al., 2012; Tsonis et al., 2018) within an empirical dynamic modelling (EDM) (Deyle and Sugihara, 2011; Takens, 1981) framework to explore signal coherence and predictability in CPUE time series across the region.

The theory behind this analysis is that fishery CPUE provides a temporally and spatially dynamic signal influenced by various process including biological (i.e., target species abundance and size composition, ecological interactions), environmental (i.e., oceanographic influences on catchability, movements, local availability of the target species), and human (i.e., targeting, gear, technology, market forces etc.). If the temporal dynamics of CPUE are consistent in space this would suggest that the processes influencing the CPUE are part of the same dynamical system. Therefore, if we can identify spatially contiguous areas of predictable CPUE time series this can indicate which series form part of the same dynamical system, and at what spatial scales different systems are operating at. Groupings of spatially coherent CPUE time series could then provide information for considering options for spatial stratification of the WCPFC bigeye and yellowfin assessments.

Detailed methodology for this component can be found in Appendix 2. Briefly, nominal catch and effort data from the 'L.BEST' Pacific Ocean pelagic longline data set between 1950-2018 inclusive, at a monthly resolution, were aggregated to a 15° × 15° Pacific-wide grid. The dataset was filtered to remove grid cells lacking consistent time series throughout the period of interest (23 out of the 83 cells), as well as observations with extreme outlier values for the effort metric - the number of hundred hooks per set (i.e., values greater than the 99th quantile value). Our final filtered dataset contained 557,260 records. Nominal catches for yellowfin and bigeye were standardised using single-species Tweedie generalised linear models (GLMs) with a log link fitted within the 'glmmTMB' package (Brooks et al., 2017) in R 4.1.1 (R Core Team, 2021).

Empirical dynamic modelling (EDM) is a non-linear statistical approach that can be used to reconstruct the dynamics of a system directly from time series data and to make forecasts about that system (Deyle and Sugihara, 2011; Takens, 1981). The method assumes nothing about the equations controlling a system's dynamics. Convergent cross mapping (CCM) uses the mathematical theory of EDM to uncover causal relationships between time series variables, allowing statements to be made on whether these variables belong to the same dynamical system (Chang et al., 2017; Munch et al., 2020, 2018; Sugihara et al., 2012).

Given previous successes in applying non-linear time series analysis and multivariate state-space reconstruction to fisheries data (Deyle et al., 2013; Glaser et al., 2014, 2011), we considered that the CCM approach may prove useful for understanding if the dynamics driving longline CPUE trends for yellowfin and bigeye are similar for certain areas across the Pacific, and if so, at what spatial scale are these trends related and predictable. By visualising the CCM results using a clustering approach we provide a means for considering spatial structures for stock assessments of bigeye and yellowfin in the WCPO.

We first tested the method using simulations under controlled settings. Working with the same 15° × 15° Pacific-wide grid described earlier, we simulated CPUE time series for each cell from a spatially explicit population dynamics model with flexibility to vary diffusion, fishing intensity, recruitment and environmental effects (i.e., sea surface temperature) on recruitment and survival (see Appendix 2). For each scenario, we then applied CCM using a set of customised functions modified from the 'rEDM' package (Ye et al., 2019) to estimate the predictability between time series pairs. The CCM output is a Euclidean distance matrix relating each time series pair. A fuzzy (probabilistic) clustering approach was applied on the resulting matrix in the 'cluster' package (Maechlaer et al., 2022) to identify and visualise the spatial patterns in time series (and hence the grid cells) that share dynamics across the region. In the simulations the method was able to reliably cluster the different CPUE time series in groups with the same dynamic properties and was able to distinguish these time series from simulated 'white noise' time series that were inherently unpredictable. The results of the simulations were used to guide settings that determine the thresholds for clustering of the CPUE time series in the main analysis of bigeye and yellowfin CPUE.

The coupled CCM/fuzzy clustering approach tested in the simulation study was applied to both the nominal and standardised longline CPUE trends for yellowfin and bigeye. The simulations indicated the importance of time series smoothness and length on CCM outcomes. Based on those analyses we decided to calculate 3-year and 5-year moving averages across the annual (raw) CPUE series (Figure 19, *Figure **21***) and compare outputs from the CCM/fuzzy clustering approach on the raw versus the smoothed trends. This resulted in six analyses per species: i) raw-nominal, ii) raw-standardised, iii) 3yr-nominal, iv) 3yr-standardised, v) 5yr-nominal, vi) 5yr-standardised.

Results

Biological information review

Appendix 1 provides detailed summary tables of the information from the various biological studies, and tagging data that were reviewed, including also spatial CPUE patterns and the SEAPODYM predictions. The relevant literature is cited in those tables. Below provides a summary of this information in relation to developing conceptual models of population structure for yellowfin and bigeye tuna.

Yellowfin tuna

Information from the larval distributions, tagging data, genetics, otolith chemistry and spatial patterns in CPUE data all provided some useful insights into population structure of yellowfin. The larval data (

Figure **2**) genetics (Appendix 1, Table 1a) and tagging data (Figure 3) all supported the hypothesis of low mixing of yellowfin tuna between the west and east Pacific populations, with a separation at around 150°W consistent with the boundary between the WCPO and the EPO assessment regions. Although tagging data indicated that that there is movement of yellowfin from the WCPO to the EPO for the larger equatorial tagging programs, movement does not appear to be extensive, which is also consistent with the limited eastward movements of yellowfin that were tagged around Hawaii (only one tagged yellowfin was documented to move from Hawaii to the EPO; Dave Itano, personal communication). Information from early studies of morphometrics and meristics along with more recent genetic studies further support separation of WCPO and EPO yellowfin populations. The CPUE patterns and SEAPODYM predictions also supported this stock separation, with a region of low predicted abundance from about 140°W to 110°W (Figure 4, Figure ***5***).

Within the WCPO the tagging data, larval abundance and CPUE patterns indicate that the adult abundance, spawning output and larval abundance are higher in the tropical equatorial region (i.e., 10°N – 10°S). Tagging shows considerable longitudinal movements throughout the tropical equatorial WCPO region, but less latitudinal movement (Figure 3), indicating high mixing across the WCPO equatorial region. Although it is difficult to know how much the low recaptures rates north and south of the tropical region is related to the lower fishing effort in the more temperate areas. Tagging data also indicated some mixing between Hawaii and Japan, between Chinese Taipei and Japan and between Chinese Taipei and the western tropical Pacific suggesting a possible migratory route following the Kuroshio Current from the tropics to southern Japan and perhaps across to Hawaii, although the CPUE is low in the region between Japan and Hawaii (Figure 4). It is notable that the only yellowfin recaptures that moved from Hawaii to Japan come from releases in the far western area of the Hawaiian EEZ at the westward portion of the Northwest Hawaiian Islands that can be influenced by the Kuroshio extension system (Dave Itano, personal communication). Movements of tagged fish between Hawaii and the western-central tropical Pacific have been observed but in very low numbers. This further supports that the population of yellowfin around Hawaii is not well mixed with the equatorial population. Fish tagged in the Coral Sea region tended to be recaptured predominantly in that area or to the north and east towards the equatorial region rather than to the south or southeast, but few fish tagged in Solomons/Papua New Guinea (PNG) region were ever recaptured on the

Australian east coast/Coral Sea area. This was supported by otolith chemistry studies that suggested most yellowfin in the Tasman Sea off eastern Australia were likely derived from the Coral Sea region.

Both tagging and CPUE patterns suggest that there is relatively low abundance of adult yellowfin in the area of the nutrient poor north Pacific sub-tropical gyre, north of about 20°N, and unlike bigeye, yellowfin CPUE was also low in the Kuroshio Current extension to the east of Japan towards Hawaii (Figure 4). The most recent otolith chemistry study provided good evidence that the majority of small (~30-40 cm) juvenile yellowfin captured around Japan originated from very small juveniles (< 10 cm) sampled further south in the western Pacific tropical region. This suggested that dispersal/movement from the equatorial western Pacific spawning areas via the western boundary currents (i.e., Kuroshio) was the most important source for juvenile recruitment around southern Japan.

While the tropical equatorial region, and western Pacific, including the Kuroshio Current region up to Chinese Taipei and the southern Okinawa islands of Japan, would appear to be a continuous area of higher yellowfin abundance, including larvae and small juveniles, information from otolith chemistry and parasites suggests a degree of isolation of the populations of juveniles in the South China Sea/Indonesian/Philippines/Vietnamese archipelagic waters and seas. Although tagging of older fish does indicate movement between these areas and the broader western Pacific and PNG/Solomons area, suggesting they are only partially isolated, perhaps more so in the juvenile stage. Connectivity of yellowfin populations between the South China Sea and the broader WCPO however remains poorly understood.

Tagging data suggests that yellowfin tagged in the PNG/Solomon Islands archipelagic seas tend to have prolonged residency and higher recaptures close to release areas compared to tag releases in more open ocean waters. This has implications for use of tag-recapture data for this area as the fish do not appear to mix more broadly into the western Pacific in sufficient numbers in a short enough time frame (recognised by the inclusion of region 8 in the 9 region model discussed above).

Finally, the spatial maps of CPUE indicate yellowfin are rarely caught outside of 40°N and 40°S. Therefore, the northern stock assessment region could be truncated to be consistent with these north-south geographic boundaries (Figure 4).

The information above and in Appendix 1, Table 1a was used to develop the conceptual model presented in Figure 6. The model based proposes four regions of the yellowfin stock in the WCPO and a separate stock in the EPO.

Bigeye tuna

Genetic studies so far provide no evidence against panmixia across the Pacific, including between the western Pacific and the South China and Philippine Seas. For bigeye the most informative biological information came from the tagging data (Figure 3), larval distributions (

Figure **2**) and growth/size at maturity information (Appendix 1, Table 1b). The spatial CPUE patterns and SEAPODYM predictions provided additional insight on regions of higher abundance (Figure 4,Figure ***5***). The tagging studies indicated that bigeye mix widely across the tropical equatorial region, but that mixing from the far west to the far east Pacific is less likely than between the central and east Pacific, supporting an isolation by distance for the far east and western pacific bigeye populations. There is significant mixing of tagged fish between the WCPO and EPO assessment regions in the central Pacific, more so than observed for yellowfin. It also appears that west-east movements from the WCPO region into the EPO region are more prevalent than in the opposite direction. Many tagged bigeye released near the eastern boundary of the WCPO are recaptured in the EPO (see also tag-recapture information in Teears et al., (2023).

The information on growth, maximum size and size at 50% maturity all lend support for a west to east cline of increasing growth rate, maximum size and size at 50% maturity. Both the tagging and growth data support an isolation by distance between the eastern EPO and the western WCPO, but a region of overlap occurs in the central equatorial Pacific. While there is no clear evidence for genetic separation of the EPO and WCPO bigeye populations, the dynamics of the EPO and the western WCPO may be relatively independent due the isolation by distance and differences in growth and recruitment sources (supported by the CPUE time series analysis, Figure 22). Spawning and larval areas are observed in the western, central and eastern Pacific, although larval abundance patterns suggest that the western Pacific region is likely more important for WCPO stock replenishment than the central or eastern Pacific, similar to yellowfin. The SEAPODYM predictions (Figure 5) suggest that larvae might be expected to be more prevalent across latitudinal bands at around 20°N and 20°S than indicated by the larval density models in

Figure **2**.

Similar to yellowfin, movement of tagged bigeye to the north and south of the tropical equatorial region appears low, although this may be influenced by the predominance of juvenile and sub-adults in the tag-recapture data, and lower fishing effort north and south of the tropical region. Bigeye tagged near Chinese Taipei also appear to move northeast along the Kuroshio Current, and some of the fish tagged off Japan were recaptured around Hawaii, with some recaptures in the tropical central Pacific. There are also occurrences of bigeye tagged in the western Pacific Ocean region that moved into the South China Sea and archipelagic waters nears the Philippines and Indonesia, suggesting a degree of mixing between these regions, consistent with the of lack genetic heterogeneity between the South China Sea and adjacent western Pacific. Similar to yellowfin, studies around Indonesia using otolith chemistry and parasites suggest juvenile bigeye remain in that area for at least the first year or so of life.

The tag recapture, SEAPODYM and CPUE patterns suggest that Kuroshio Current and its extension towards Hawaii, may facilitate bigeye movement across the northern WCPO between Japan and Hawaii. The relative CPUE in the Kuroshio current extension was notably higher for bigeye than yellowfin, consistent with the observations of good bigeye catches off the Sanriku coast which is a known prominent fishing ground for bigeye for Japanese longliners during winter. Consistent with yellowfin the CPUE indicates that bigeye are really only caught between 40°N and 40°S (Figure 4).

Finally, while bigeye from the Coral Sea tagging were often recaptured in the tropical equatorial region of the western and central Pacific there was little indication that tagged bigeye from the tropical equatorial region were moving to the east Australian coast/Coral Sea (Figure 3).

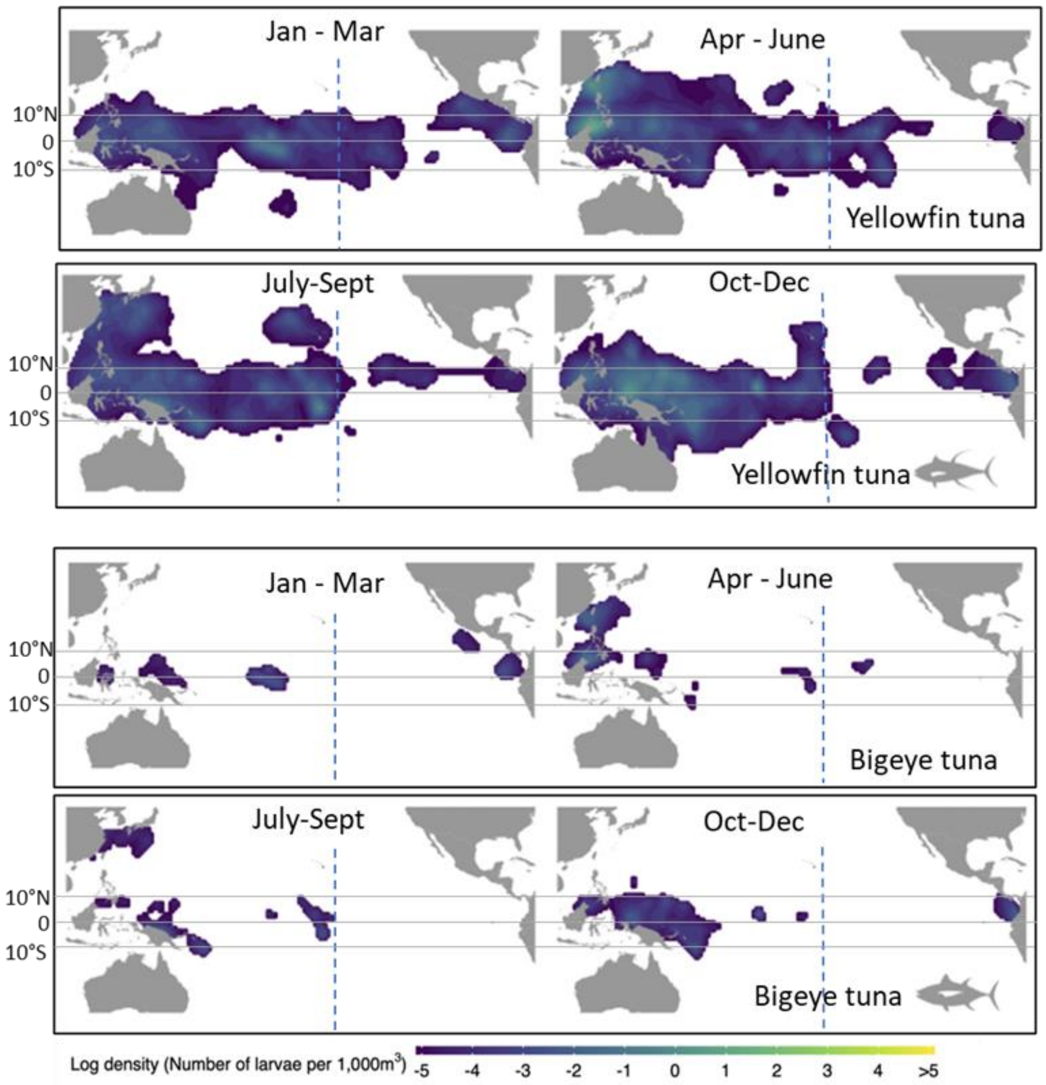

Figure 2 Maps showing seasonal yellowfin and bigeye larval densities across the Pacific for the period 1960-1985 from geostatistical modelling of the Nishikawa data set by Ijima and Jusup (2023). https://doi.org/10.48550/arXiv.2304.09442

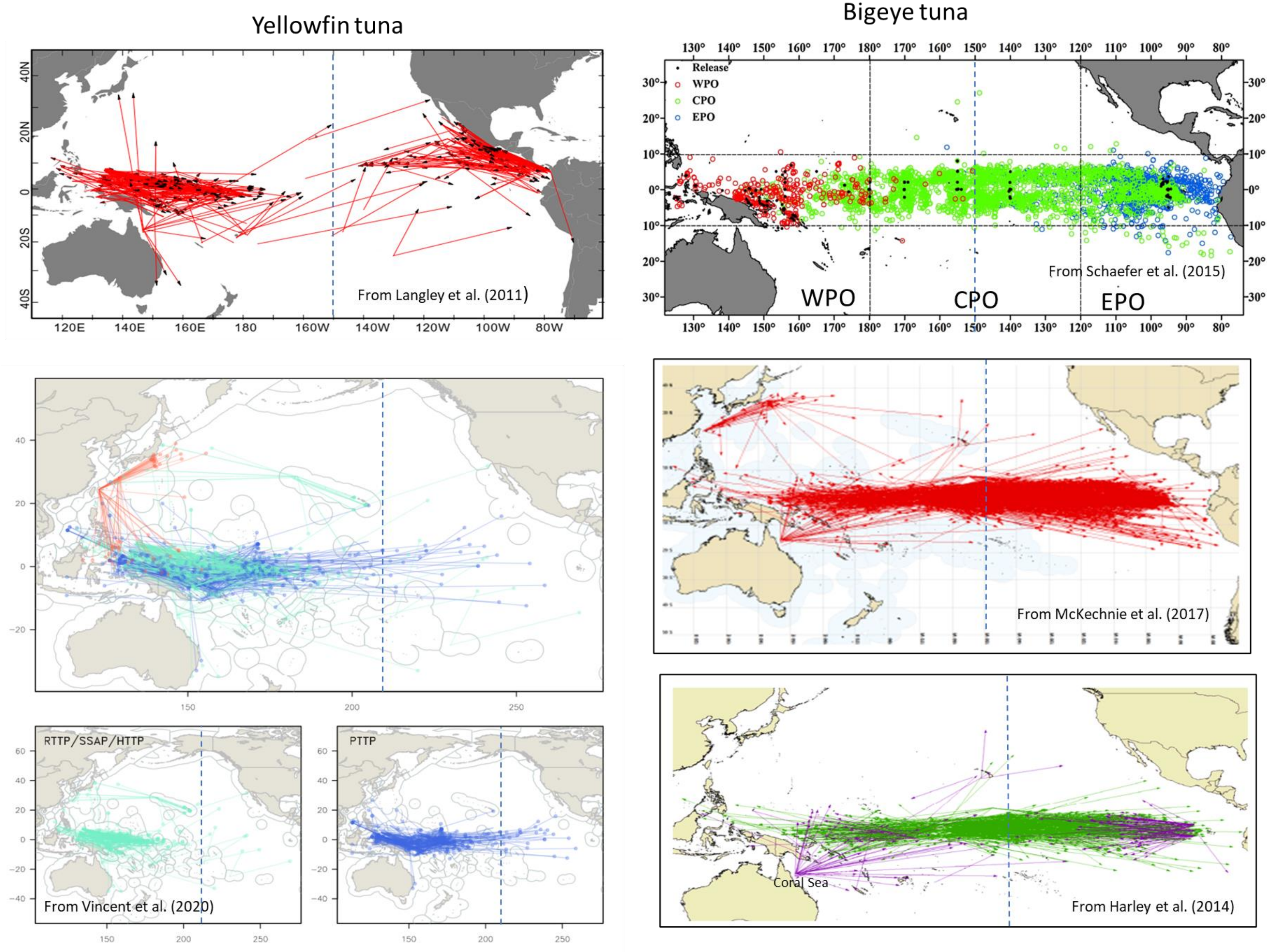

Yellowfin tuna

Bigeye tuna

From Langley et al. (2011)

From Schaefer et al. (2015)

From Vincent et al. (2020)

From McKechnie et al. (2017)

From Harley et al. (2014)

Figure 3 Maps of tag recapture displacements for yellowfin (left panels) and bigeye (right panels) that moved more than 1000 nm. Top right panel from Schaefer et al. (2015) shows recapture locations of bigeye released in the western Pacific Ocean-WPO, central Pacific Ocean-CPO, and eastern Pacific Ocean-EPO. Vertical blue dashed line at 150°W is border between WCPO and EPO assessment regions.

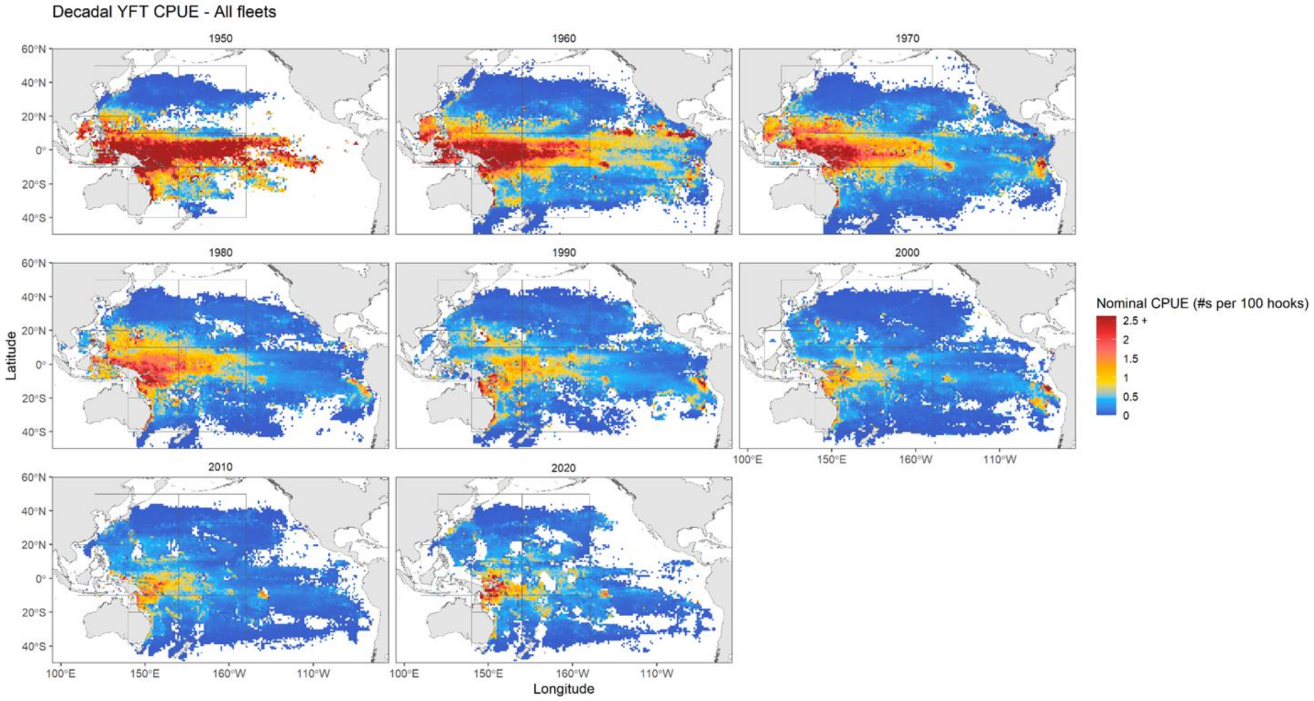

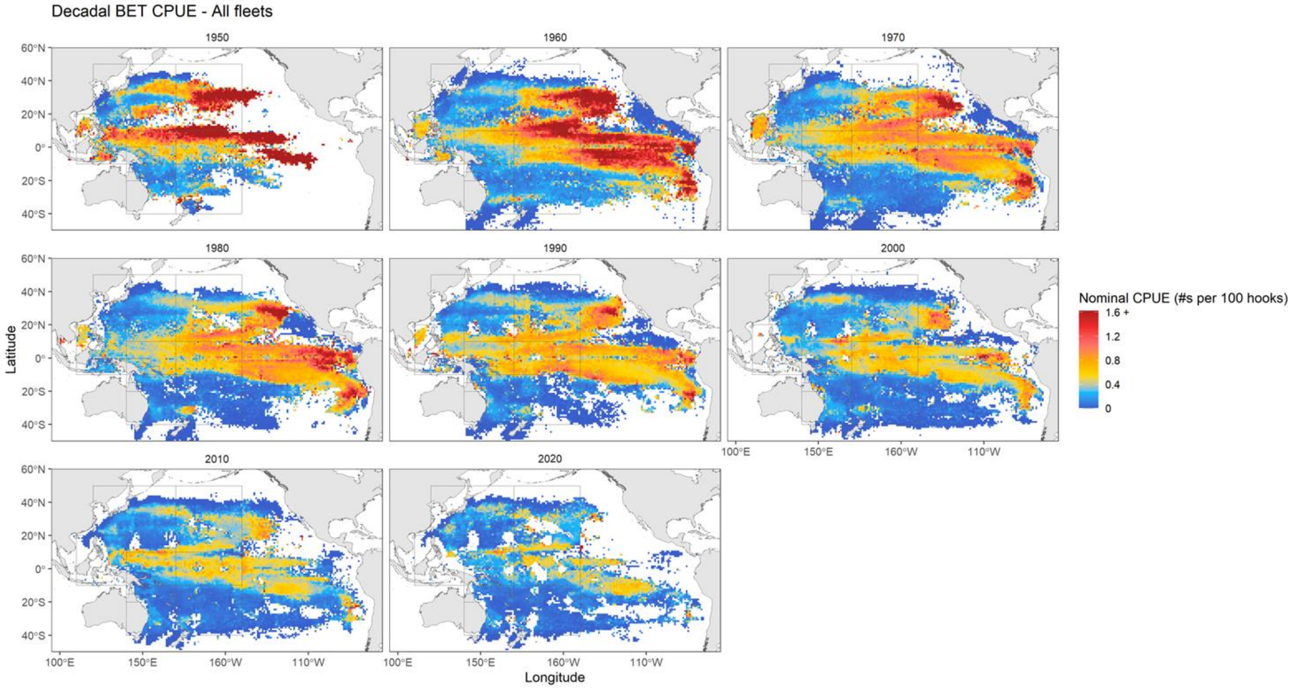

Figure 4 The decadal distributions of yellowfin (top) and bigeye (bottom) tuna nominal CPUE (numbers per 100 hooks fished) across all fishing fleets in the Pacific wide operational longline data set (from Teears et al. 2023).

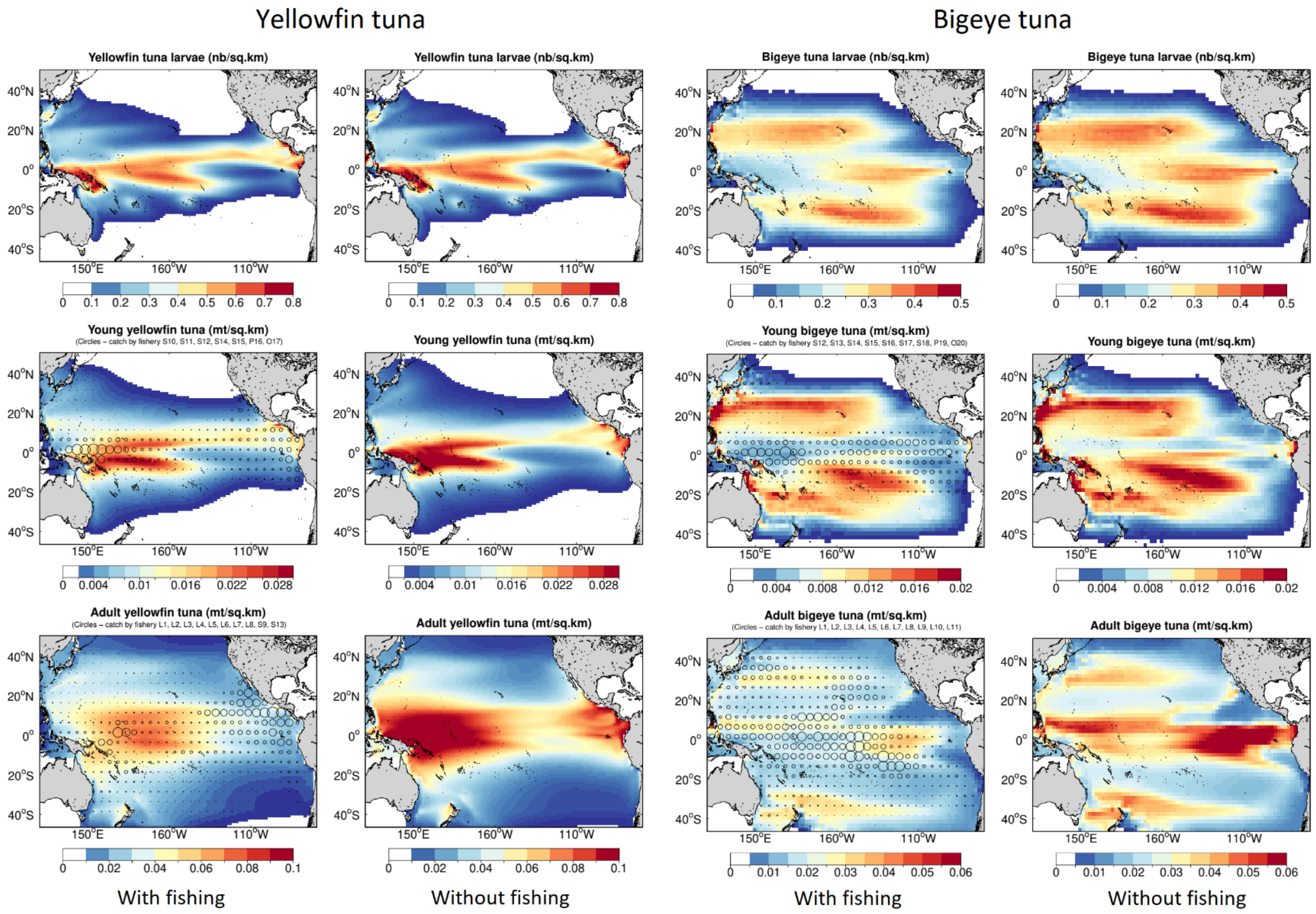

Figure 5 SEAPODYM plots (left – yellowfin, right - bigeye): from top to bottom: average density of larval (Nb/km^2), young (mt/km^2, including all age classes younger than age at 50% maturity) and adult (mt/km^2, including all age classes older than age at 50% maturity) tuna predicted with (left) and without fishing (right). Open circles indicate catch distributions aggregated at 5x5 degree. From Senina et al., (2023).

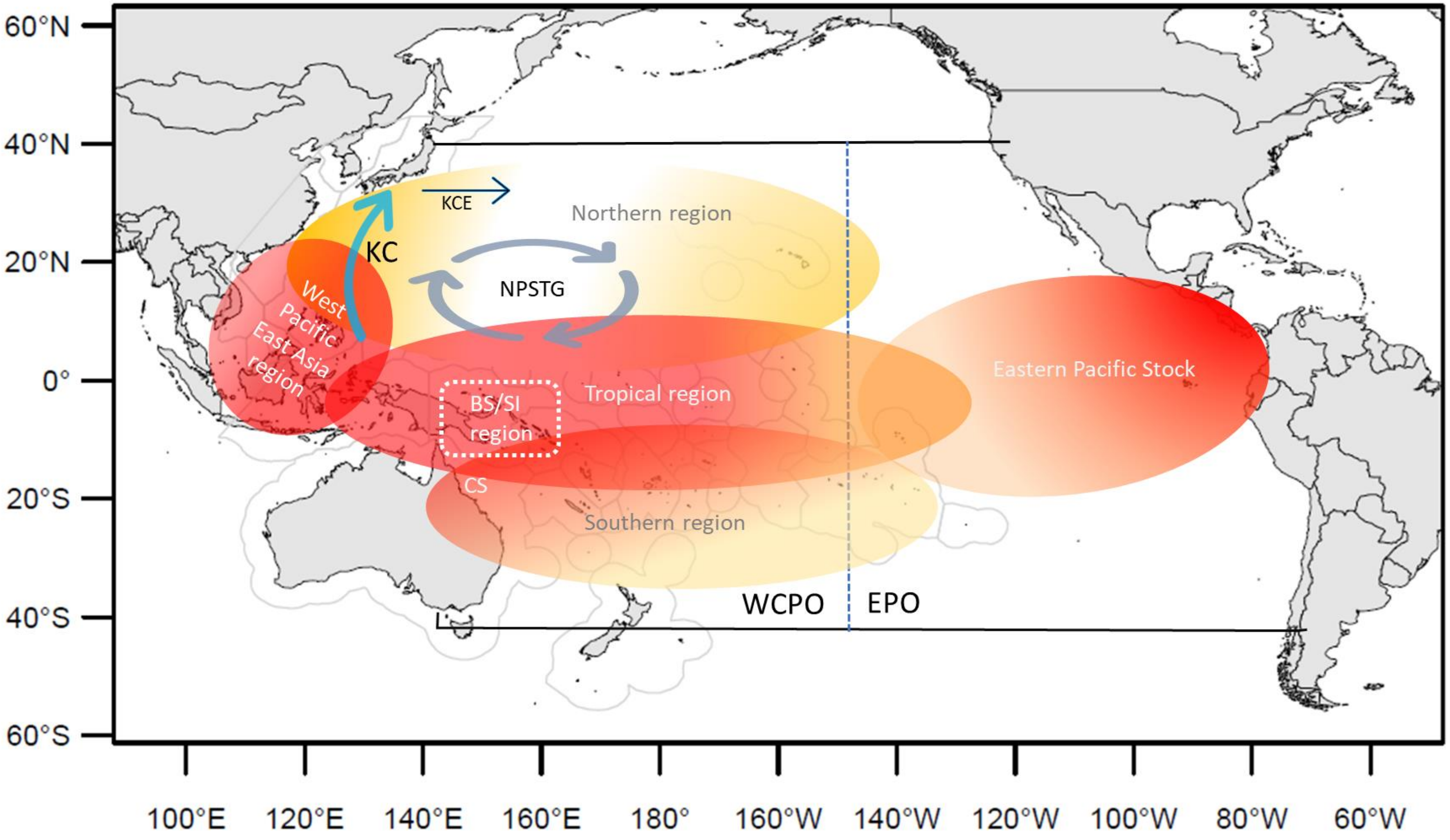

Figure 6 Conceptual model of broad yellowfin population regions based on the information discussed in Appendix 1 Table 1a, with proposed four subregions for the yellowfin tuna stock in the WCPO and a separate stock in the EPO, plus the archipelagic waters region of the Bismarck Sea/Solomon Islands. The colour shades reflect 'general' relative abundance of adults, redder = higher abundance. CS=Coral Sea, BS = Bismarck Sea, SI=Solomon Islands. WCPO=Western and Central Pacific Ocean assessment area, EPO=Eastern Pacific Ocean assessment area, KC = Kuroshio Current, KCE=Kuroshio Current Extension, NPSTG=North Pacific Subtropical Gyre.

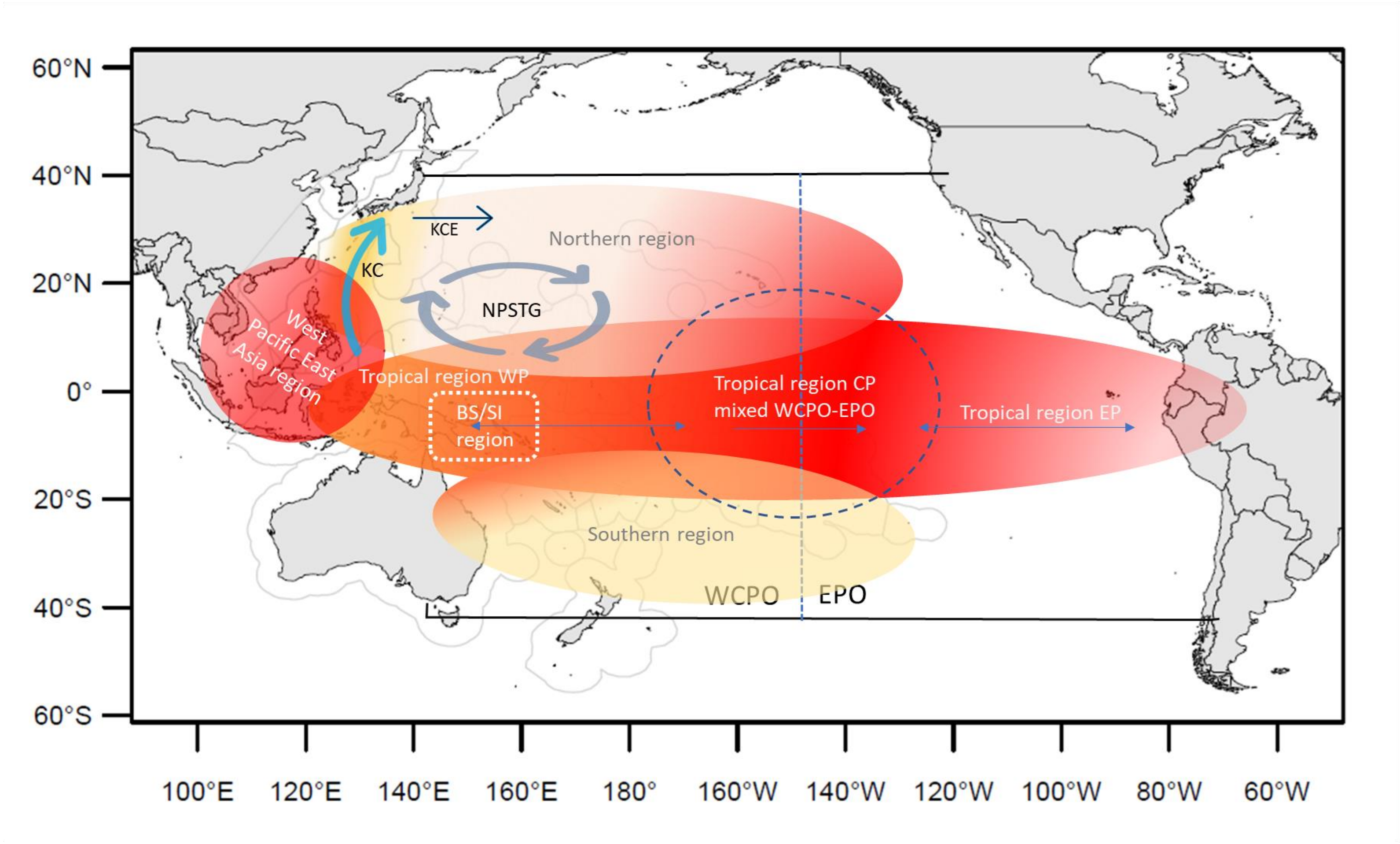

Figure 7 Conceptual model of broad bigeye population regions based on information discussed in Appendix 1 Table 1b, with proposed four subregions for the bigeye tuna stock in the Pacific and a region of overlap between the WCPO and EPO (isolation by distance across the equatorial zone), plus the archipelagic waters region of the Bismarck Sea/Solomon Islands. Arrows in tropical region indicate predominant tag movements. The colour shades reflect 'general' relative adult abundance, redder = higher abundance. CS=Coral Sea, BS = Bismarck Sea, SI=Solomon Islands. WP=Western Pacific, CP=Central Pacific EP=Eastern Pacific, KC = Kuroshio Current, KCE=Kuroshio Current Extension, NPSTG=North Pacific Subtropical Gyre, WCPO=Western and Central Pacific Ocean assessment area, EPO=Eastern Pacific Ocean assessment area.

Size composition analysis

Size data

The number of longline LF and WF records each year varied throughout the study period (Figure *8*). The number of records by species were however similar each year for the particular data type. The number of WF observations for both species declined from the early 2000s. This decline relates to decreases in WF samples collected by the Japanese fleet in particular. Conversely, the number of LF observations increased over this same period for both species due to increased sampling by distant water and Pacific Island fleets. Both the WF an LF data show a sharp decline in sample numbers starting 2020, which is due to the impact of COVID on the sampling programs and for 2022 the data were incomplete at the time of this analysis.

Spatial LF (Figure 9, Figure ***10***) and WF histograms (Figure 11, Figure ***12***) are presented for LL data by each grid cell. In general, LF data had better spatial coverage than the WF data, however many grid cells were not sampled. WF data, especially in the northwest and far south, fell into 'columns', suggesting these data were collected/aggregated at a coarser spatial scale than analysed (e.g., possibly 10 x 10° grid cells).

Mean length and weight per 5° x 5° grid cell are presented in Figure 13 and Figure ***14*** for yellowfin and bigeye respectively. Mean length and mean weight for bigeye suggests longer and heavier fish are caught in the equatorial region. This spatial pattern isn't as clear for yellowfin data, where the top north-eastern region around Hawaii (lat. 25-40°, long. 190-210°, Figure 13) seems to have heavier/longer fish captured compared to the rest of the study region.

Regression tree splits

The cumulative increase in percentage variance (%var) explained with increasing number of splits is presented in Figure 17 andFigure ***18*** for the length and weight frequency analyses respectively. Percentage variance explained was higher for bigeye than yellowfin for both the LF and WF. LF data for bigeye had the highest percentage variance explained, rapidly increasing to >20% after two splits. The rate of increase in %var with increasing splits for YF reduced after 5 splits (top panel), and did not exceed 20% for the LF or WF.

While increasing the splits in a regression tree might lead to increased variance explained, it does not necessarily lead to useful divisions of the data. Adding more splits can start to identify noise and create patchy groupings that would not be informative, practical or meaningful for the purpose of these analyses. There are no hard and fast rules for determining when to stop splitting in regression tree analysis and a level of pragmatism is required. In this case we are building a weight of evidence for spatial stratification of a stock assessment. Splitting further after three splits started to produce impractical and unlikely meaningful groupings, such as the narrow zone 3 band for the bigeye LF analysis (Figure 16). We felt that three splits was a reasonable and pragmatic point to stop splitting for the purpose of this analysis.

The results of the regression tree analysis based on three splits (i.e., creation of four zones) are presented in Figure 15 (yellowfin) and Figure 16 (bigeye). Regardless of species and data type (LF versus WF), there is consistent grouping of the equatorial region (zone 2 in Figure 15Figure 16). For three of the four analyses this equatorial region includes the cells from 10°N – 5°S, and in the fourth (yellowfin WF), it extends from 15°N – 10°S. Similarly, irrespective of species, LF or WF, a continuous southern region is identified (zone 1 in Figure 15Figure 16). For cells north of the equatorial region there was some variation in the groupings among the analyses. For yellowfin tuna there were two northern zones identified (zones 3 and 4), with slight difference between the LF and WF in the east-west longitudinal split at around 175 ° (Figure 15). This appeared related to the larger yellowfin observed in the data from around Hawaii. For the bigeye analysis, the LF data did not indicate a northern region longitudinal split but had a narrow zone at 10-15°N, whereas for the WF data there was a longitudinal split at 145° (Figure 16), although we note that WF data are patchy in this region of the analysis (Figure 12).

Upon inspection of the data grouped for the zones produced by the three splits for each analysis we note that the LF and WF histograms for each zone do not exhibit characteristics of unmodelled heterogeneity (i.e., no bimodality or 'shoulders' in the distributions are observed) (Figure 17Figure 18). This suggests that this number of splits was sufficient to capture the region-wide differences in LF and WF distributions and supported the decision to stop splitting at three splits.

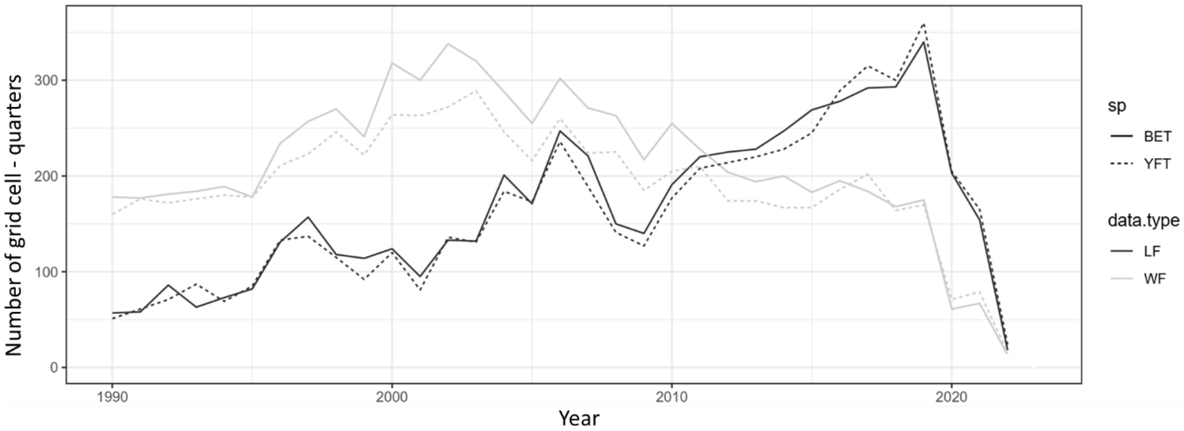

Figure 8 Annual time series of the numbers of 5° x 5° x quarters grid cells with available length frequency (LF) and weight frequency (WF) data for the analysis from 1990 – 2022 for yellowfin (YFT) and bigeye (BET) tuna. Dark lines are LF and light grey lines are WF.

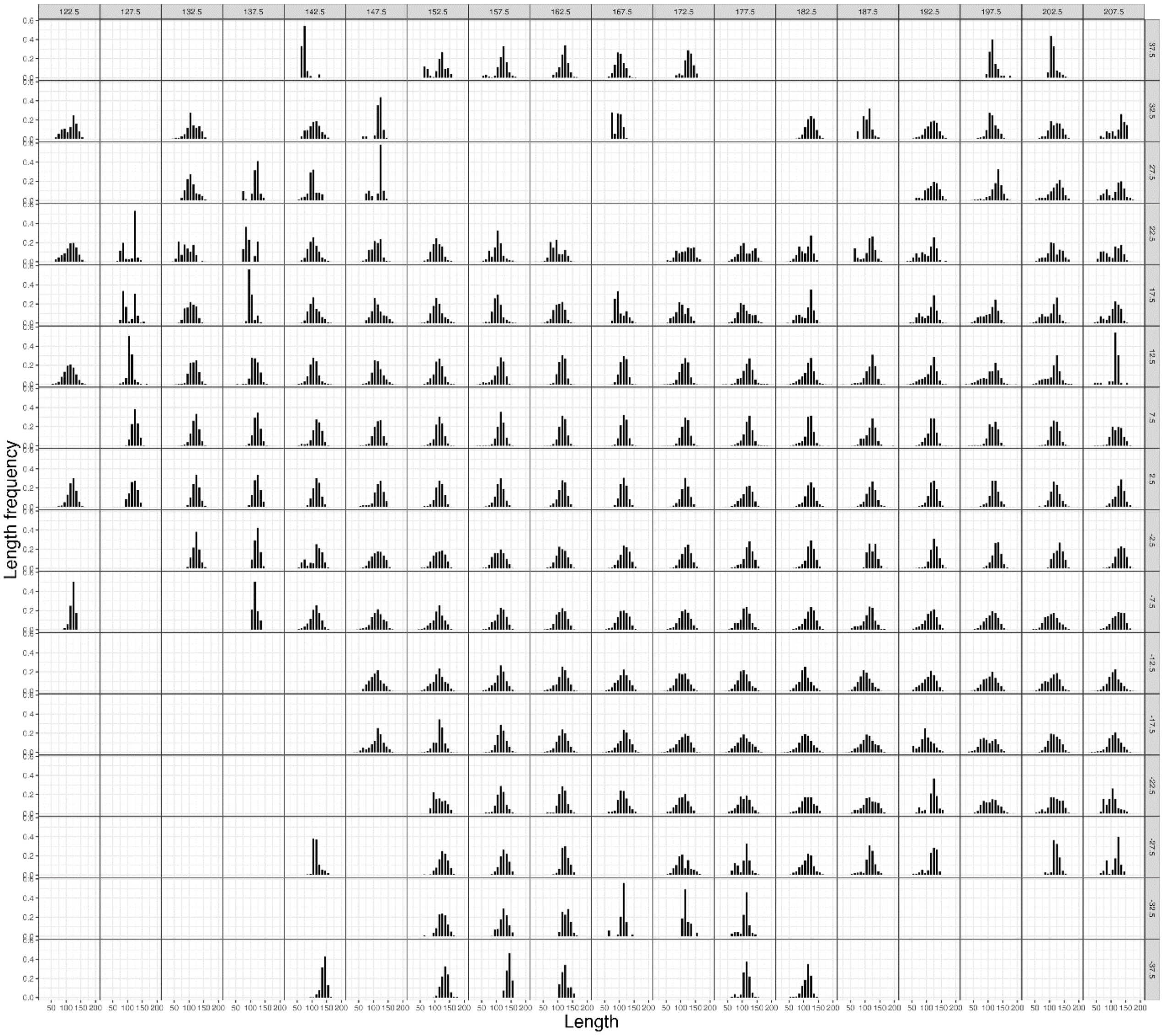

Figure 9 Yellowfin tuna: length frequency histograms for each 5° x 5° grid cell.

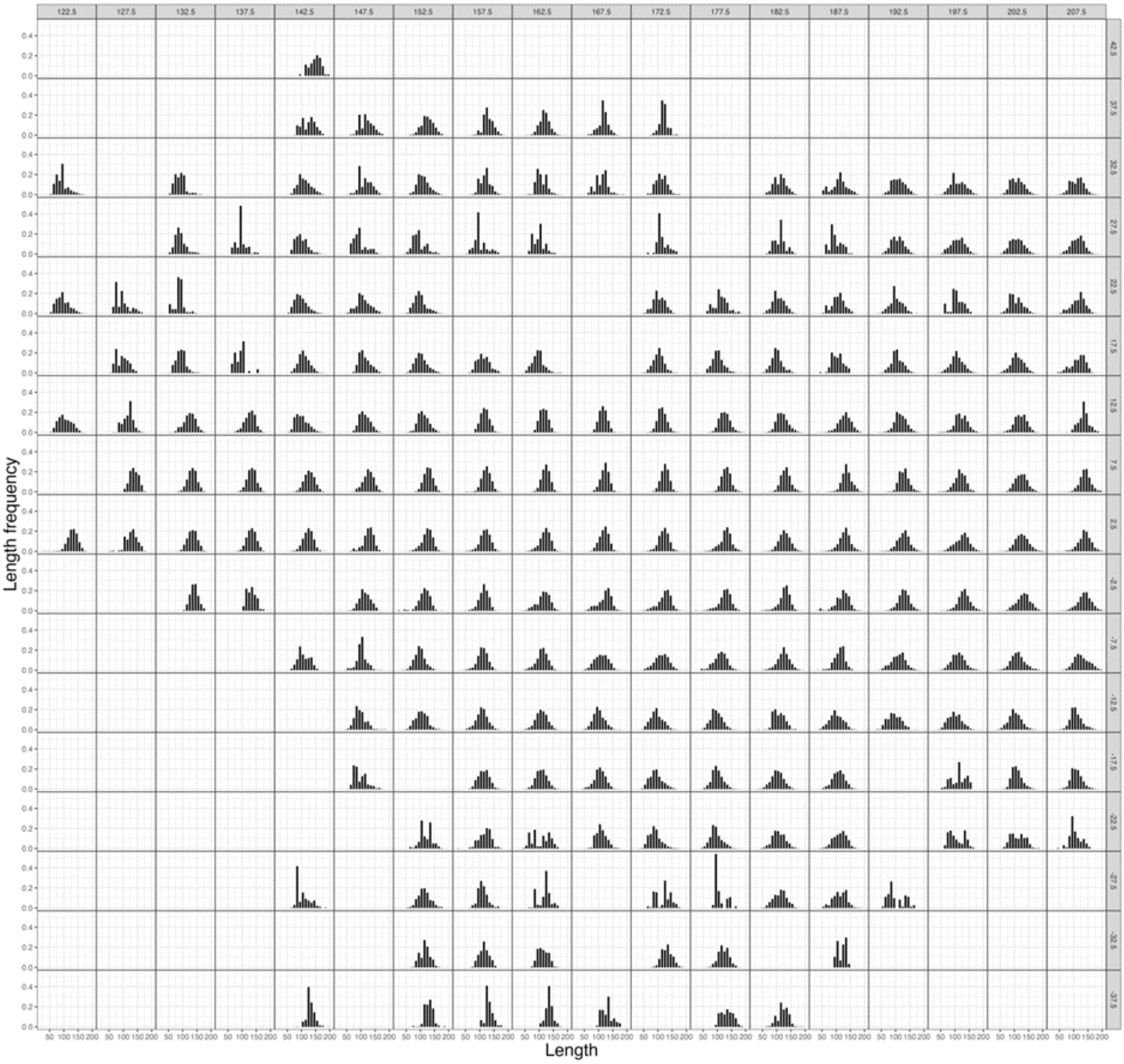

Figure 10 Bigeye tuna: length frequency histograms for each 5° x 5° grid cell.

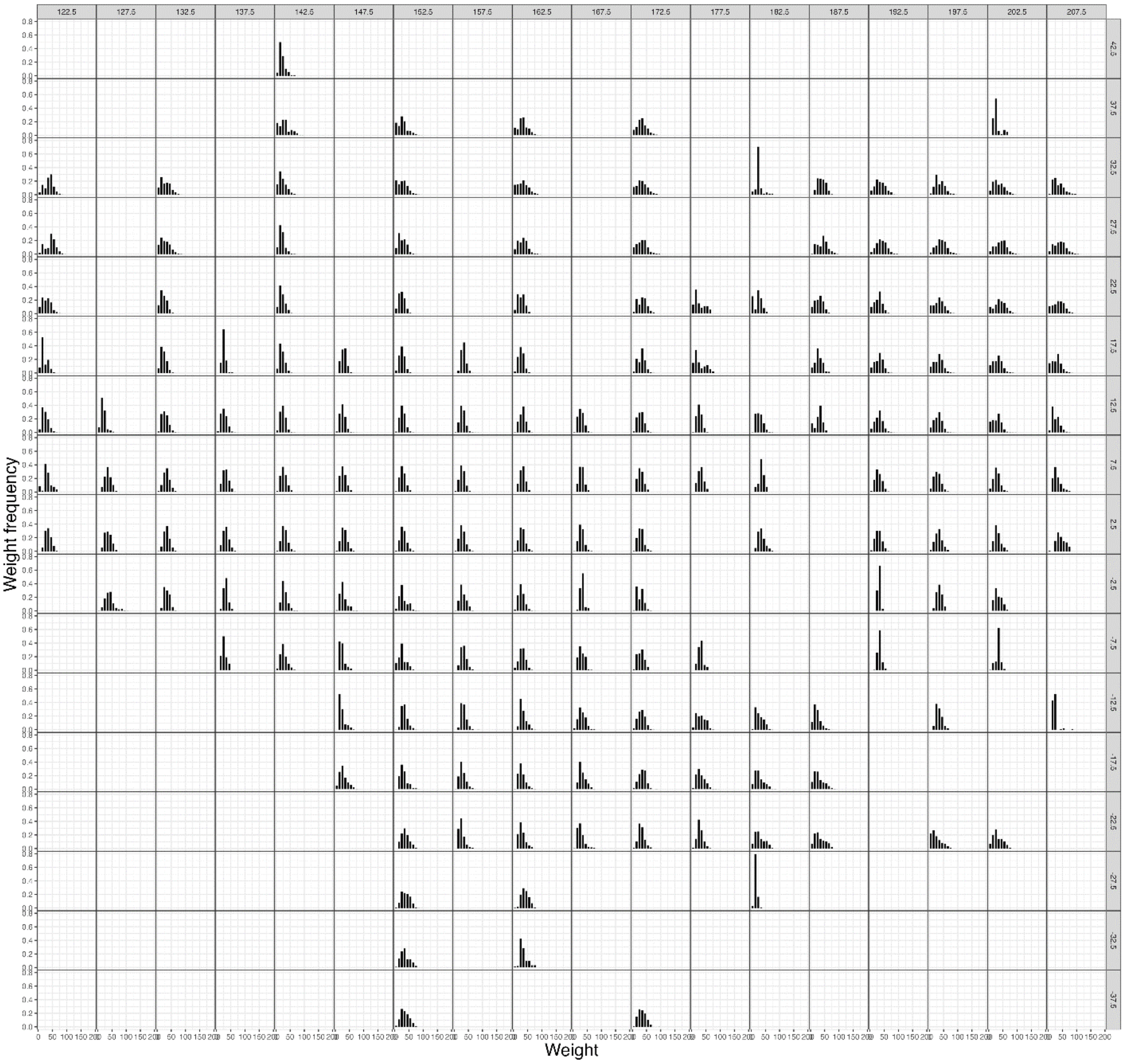

Figure 11 Yellowfin tuna: weight frequency histograms for each 5° x 5° grid cell.

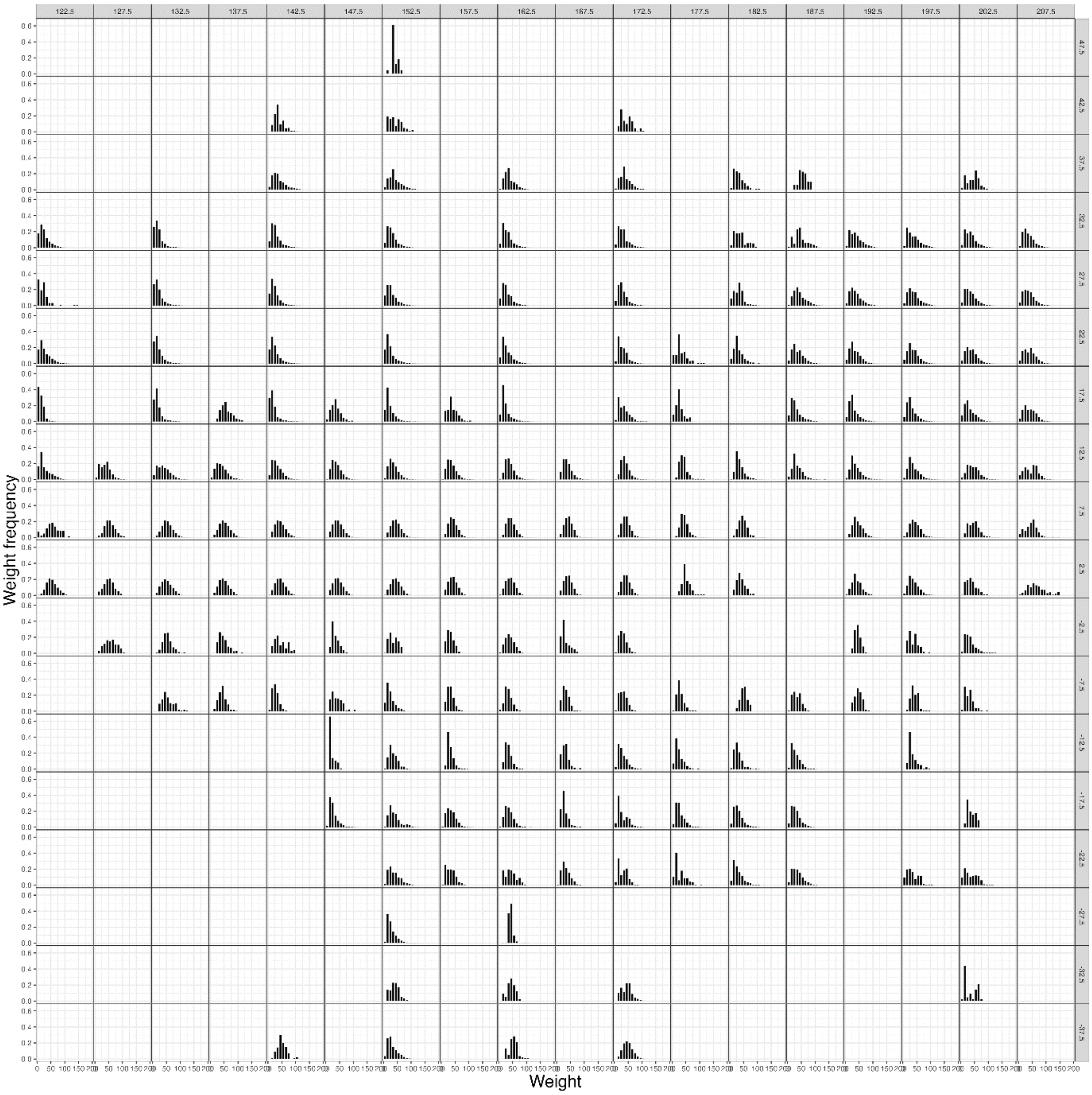

Figure 12 Bigeye tuna: weight frequency histograms for each 5° x 5° grid cell.

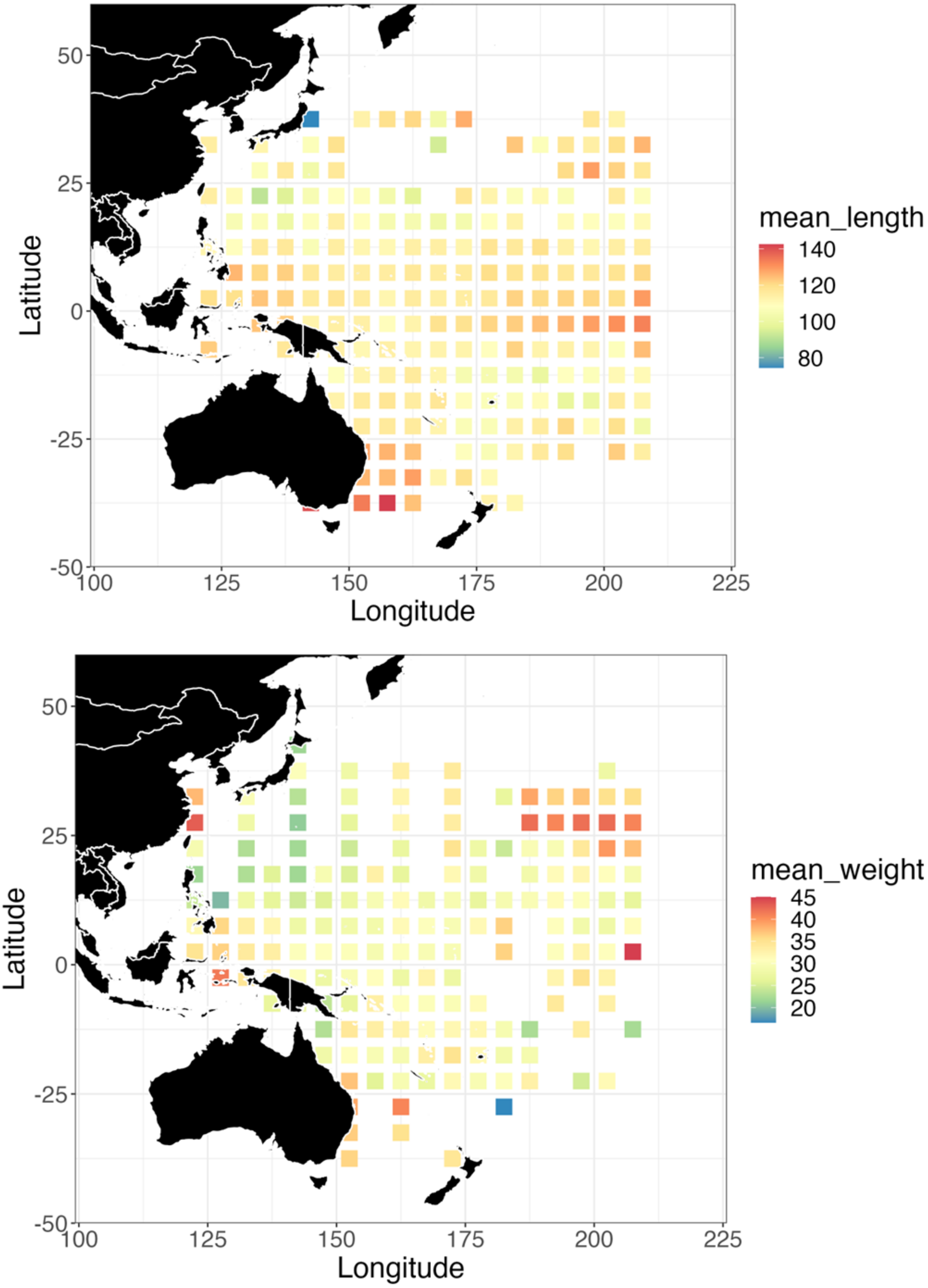

Figure 13 Yellowfin tuna: Mean lengths (top) and mean weights (bottom) for each 5° x 5° grid cell.

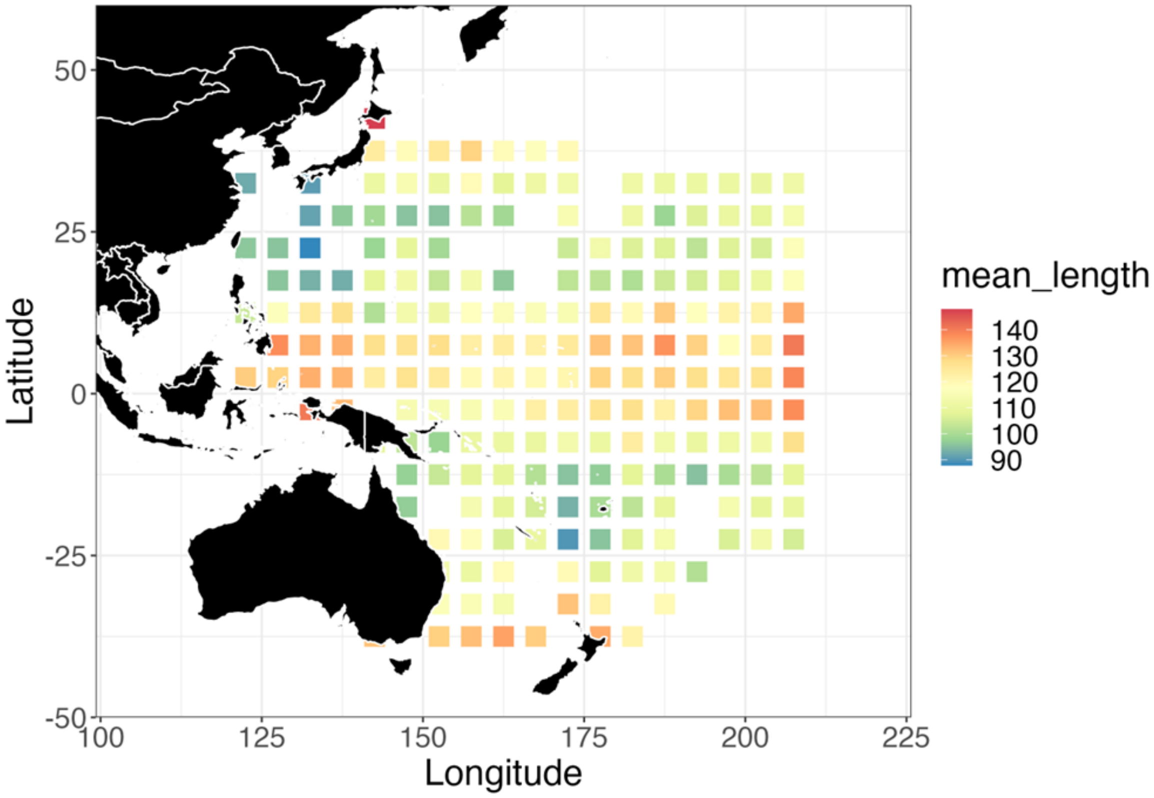

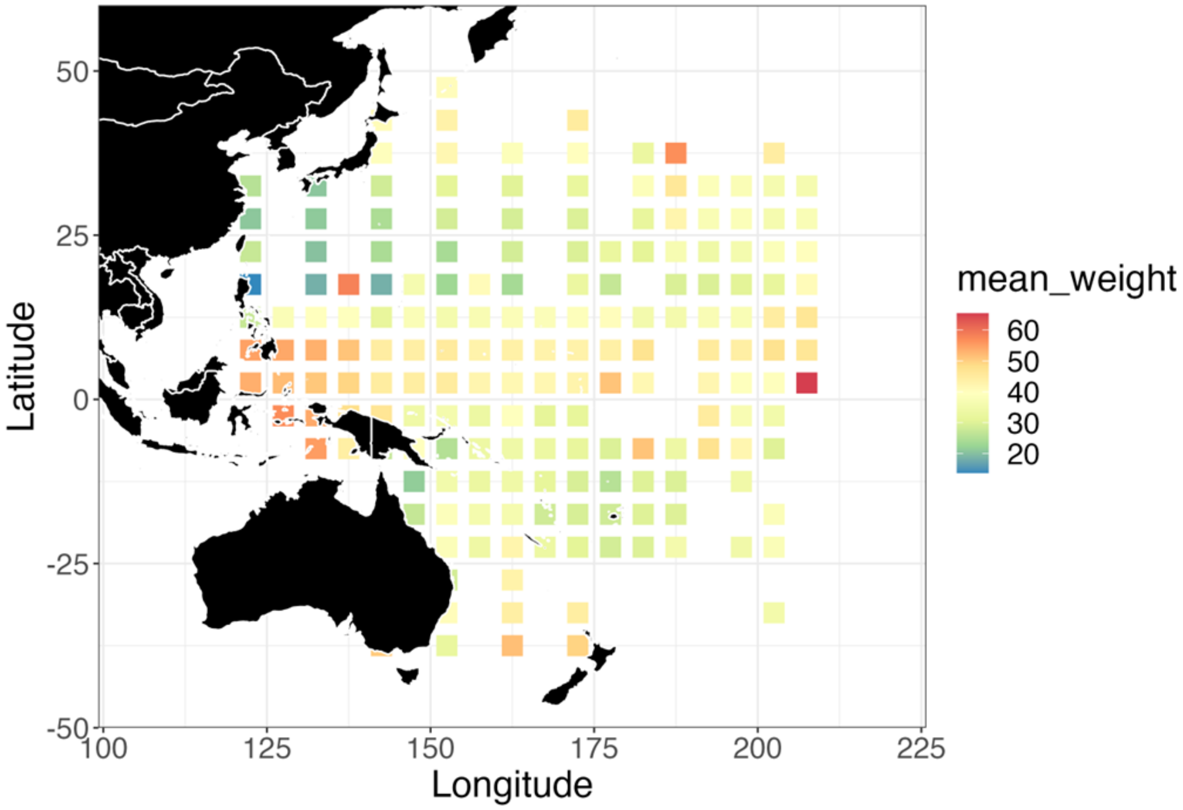

Figure 14 Bigeye tuna: Mean lengths (top) and mean weights (bottom) for each 5° x 5° grid cell.

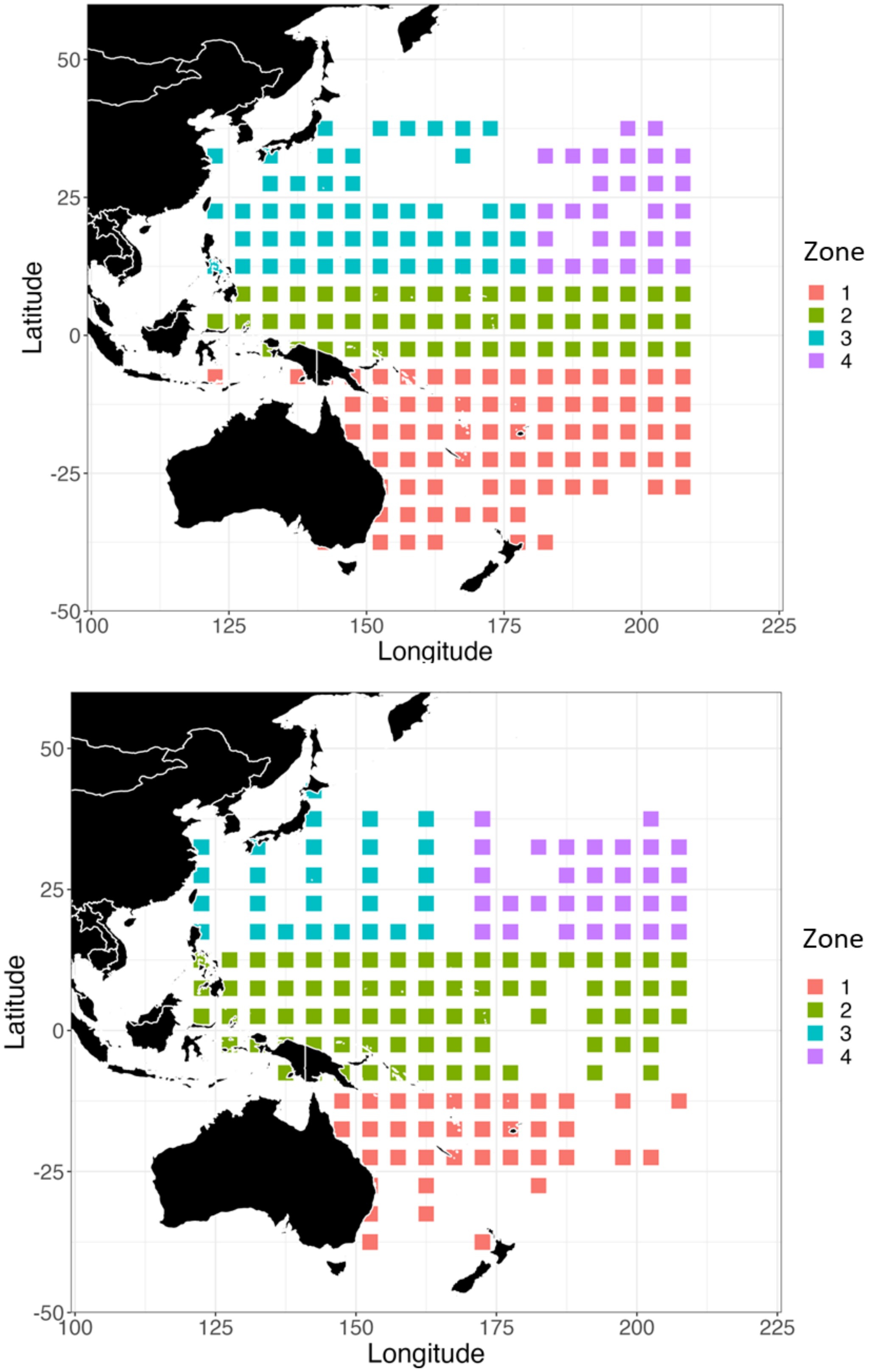

Figure 15 Yellowfin tuna: result of regression tree analysis showing the zonal groups after 3 splits for length frequency (top) and weight frequency (bottom).

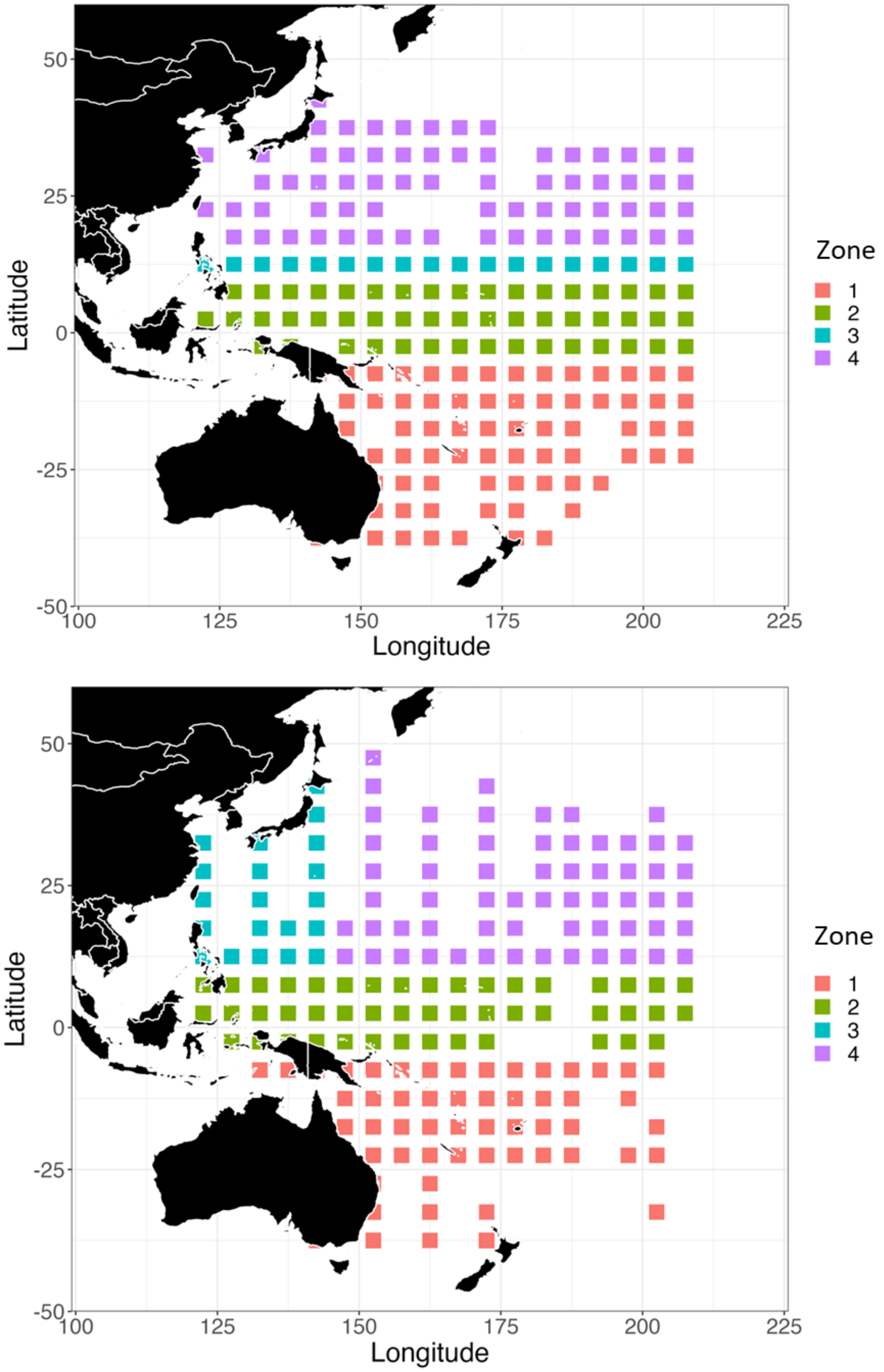

Figure 16 Bigeye tuna: result of regression tree analysis showing the zonal groups after 3 splits for length frequency (top) and weight frequency (bottom).

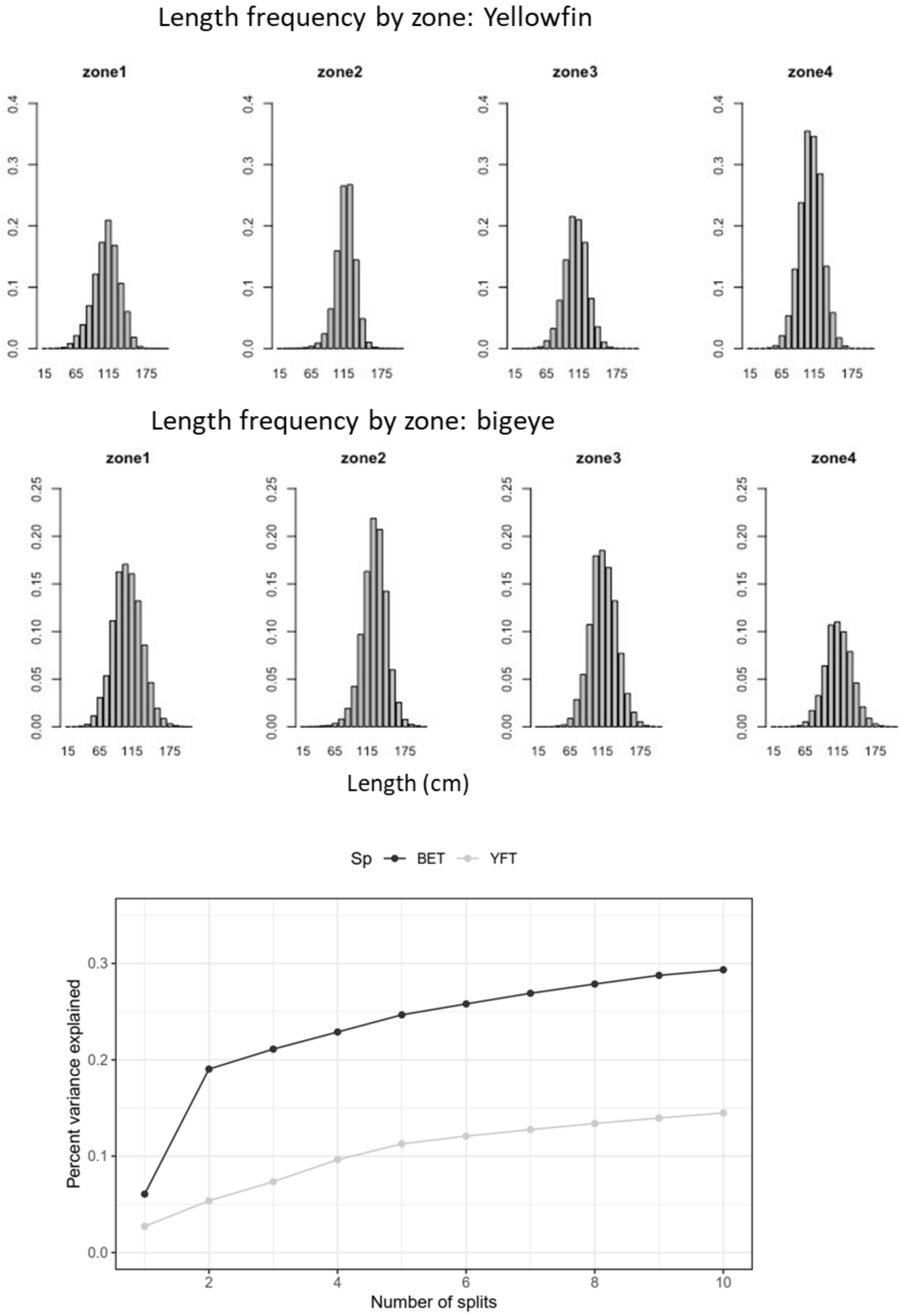

Figure 17 Plots of length frequencies for the four zonal groups after three splits in the regression tree analyses for yellowfin (top) and bigeye (second from top), and the cumulative variance explained after successive splits in the analyses (bottom).

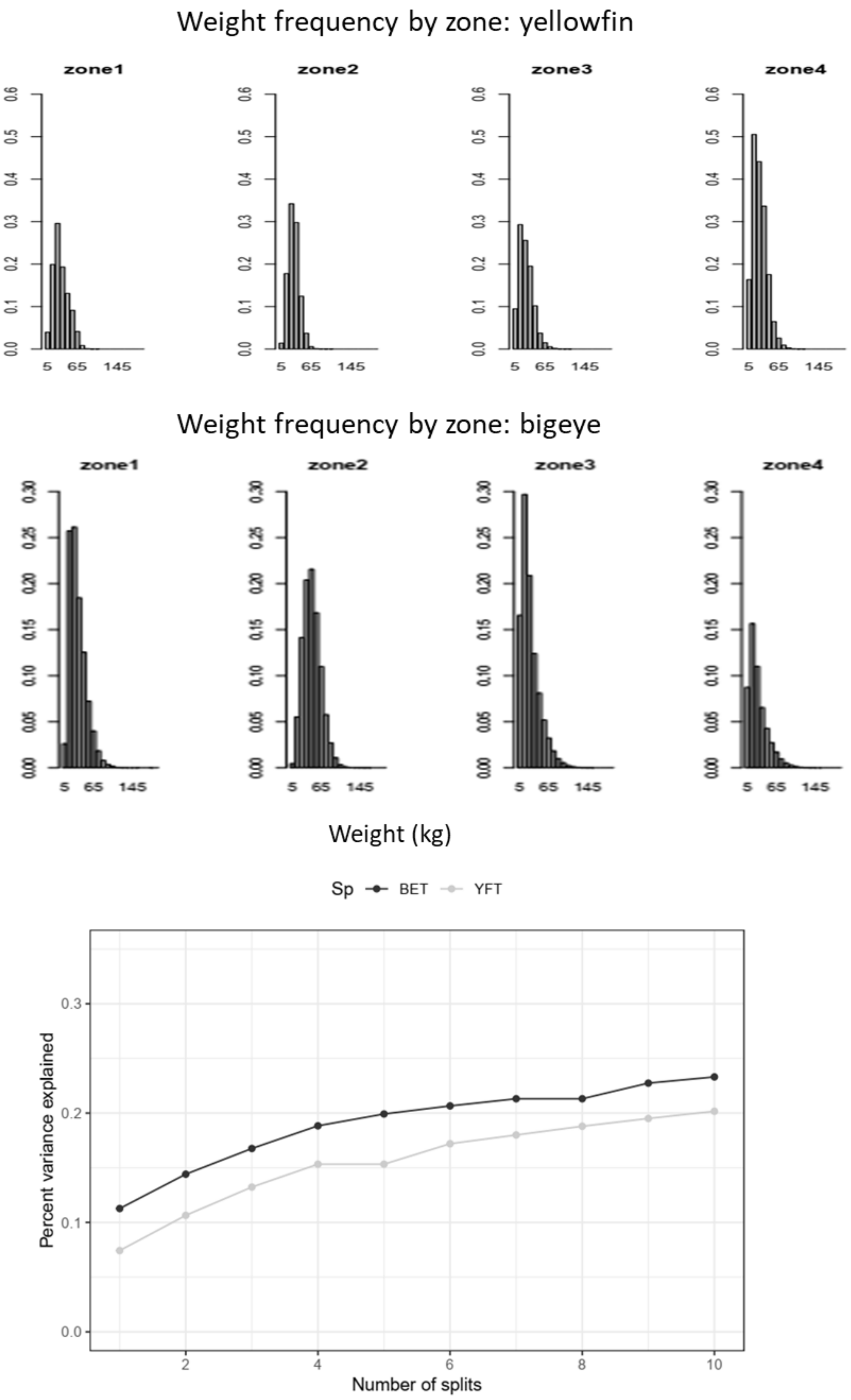

Figure 18 Plots of weight frequencies for the four zonal groups after three splits in the regression tree analyses for yellowfin (top) and bigeye (second from top), and the cumulative variance explained after successive splits in the analyses (bottom).

CPUE time series analysis

Yellowfin

The standardised CPUE time series mostly tracked the nominal CPUE trends across the region, although standardisation did reduce the magnitudes of some spikes in the nominal CPUE (Figure 19). However, nominal and standardised CPUE time series (Figure 19 – left panel) were characterised by substantial year-to-year spikiness, particularly in more southern and northern regions (i.e., grid cells 26 to 38, and 68 to 75).

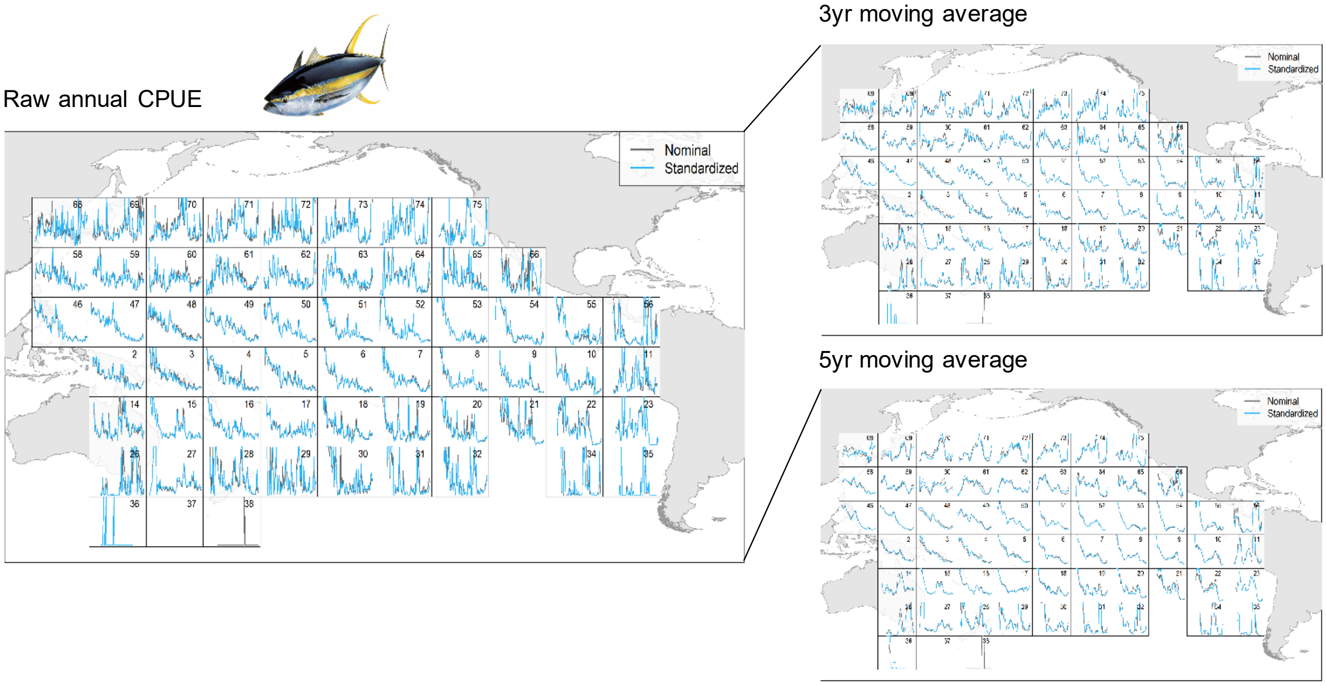

Figure 19 Nominal (black) and standardised (blue) longline CPUE time series for yellowfin tuna between 1950 and 2018, inclusive, aggregated to a 15° × 15° grid. Left panel: raw annual time series; top right panel: with a 3-year moving average applied; bottom-right panel: with a 5-year moving average applied. Grid cell ids are numeric references for the CCM/clustering approach.

Excessive spikiness can be problematic for CCM analysis, hence we also explored the application of 3- and 5-year moving averages. We found that smoothing the raw CPUE series did influence the outcomes of the CCM/clustering approach for the yellowfin data. The most consistent results were achieved using the 3-year moving average time series (Figure 19). This seemed to provide the best compromise between dampening the impact of larger spikes in the raw CPUE series whilst retaining key dynamics needed to inform the CCM predictions. Hence, we focus here on results for the '3yr-nominal' and '3yr-standardised' analyses.

Five clusters were identified by the 3yr-nominal analysis and four clusters by the 3yr-standardised analysis (Figure 20). Most clusters were characterised by a series of contiguous grid cells assigned with high probability to the cluster they were placed in. Clearly defined central north Pacific (Figure 20 e) nominal and d) standardised) and eastern Australian [Figure 20 – cluster d) nominal and cluster c) standardised] clusters were identified in both analyses. The 3yr-standardised analysis incorporated the two equatorial clusters that were evident in the 3yr-nominal analysis [Figure 20 – clusters a) and b) nominal and cluster a) standardised]. Both analyses returned one spatially patchy cluster containing cells whose dynamics most closely matched a white noise process [Figure 20 – cluster c) nominal and cluster b) standardised].

3yr-nominal analysis - yellowfin

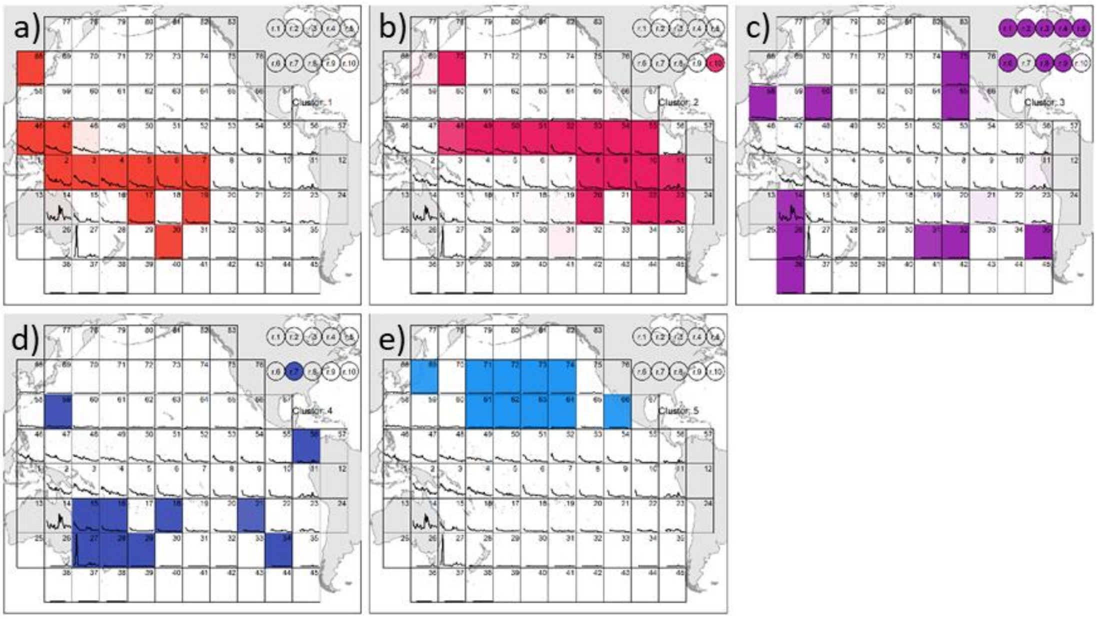

3yr-standardised analysis - yellowfin

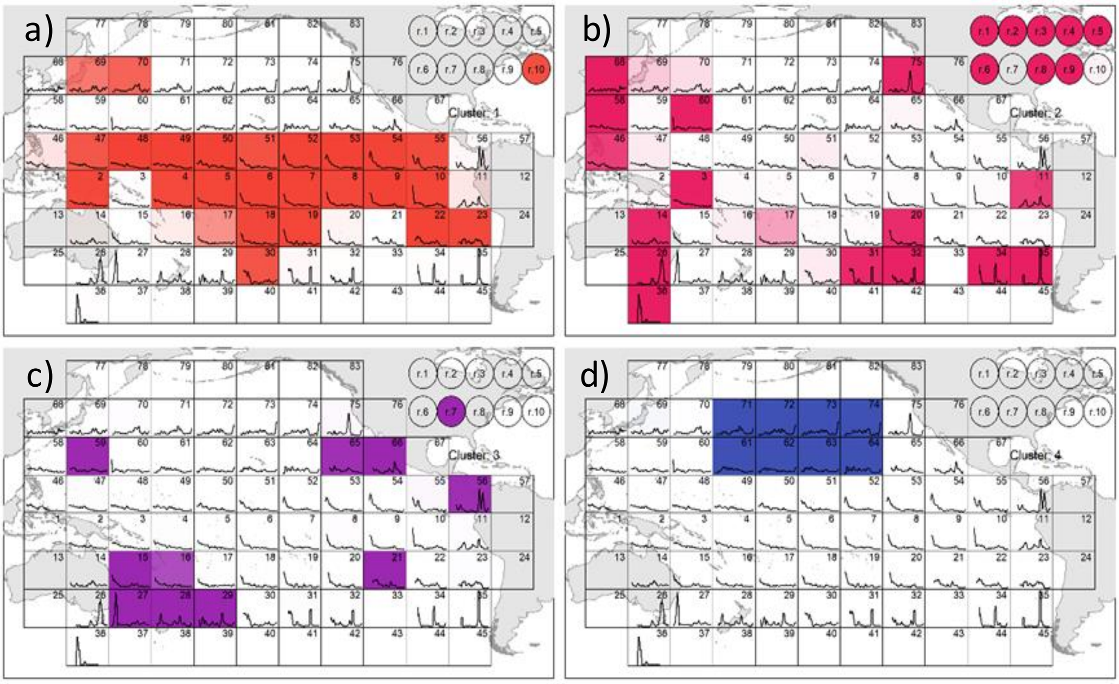

Figure 20 Results from the CCM/fuzzy clustering approach for the '3yr-nominal' (top panel) and '3yr-standardised' (bottom panel) analyses for yellowfin. Black lines in each 15° × 15° grid cell are 3-year moving average CPUE time series for yellowfin between 1950-2018 (note the different y-axis scale compared with Figure 19). Other information as for Figure 19. Note the allocation of colours to clusters is not comparable between the nominal and standardised figures. Within each cluster the lighter the shade indicates the lower the strength of the relationship between that cell and the other cells.

While the mechanisms underpinning these 'white noise' or unpredictable cells require further exploration, for the present analysis, we consider that clusters linked closely to the white noise time series are unlikely to be reflective of human and/or ecological influences on the longline fishery system and are not considered informative for spatial stratification of the stock assessment, however they still indicate differences between these cells and the other more contiguous clusters.

The results for yellowfin appear to indicate plausible structure in that the yellowfin longline CPUE dynamics that are somewhat consistent with the results from the size composition analysis (Figure 15), i.e., a north central Pacific region, an equatorial region and a southern region. Overall, the analyses provide some support for a single southern region, one equatorial region and one or two northern regions within the WCPFC Convention Area.

Bigeye

As for the yellowfin data, the standardised CPUE time series for bigeye generally traced the main trends in nominal CPUE patterns, but the standardisation tended to have stronger effects in the cells to north west of the study region (Figure 21, cells 58, 59, 60, 69 70). The raw annual time series (Figure 21– left panel) in some grid cells were characterised by strong year-to-year fluctuations, particularly in the northwest (i.e. grid cells 58, 68, 69), south (i.e. grid cells 14 to 35) and east (e.g. grid cells 55, 56, 66). As with yellowfin we applied moving averages to reduce the magnitude of these spikes (Figure 21 – right panels) but retain key features of the time series dynamics.

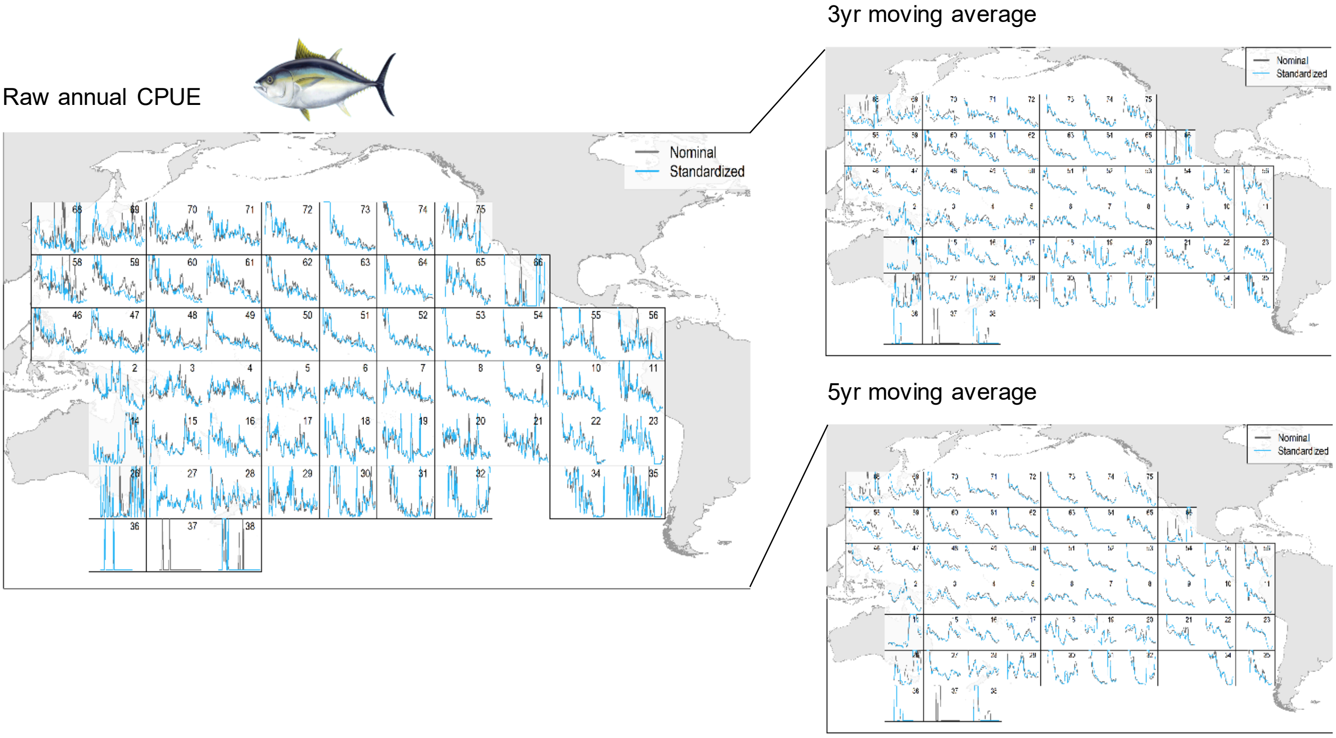

Figure 21 Nominal (black) and standardised (blue) longline CPUE time series for bigeye tuna between 1950 and 2018, inclusive, aggregated to a 15° × 15° grid. Left panel: raw annual time series; top right panel: with a 3-year moving average applied; bottom-right panel: with a 5-year moving average applied. Grid cell ids are numeric references for the CCM/clustering approach.

Similar to the yellowfin analyses, we found slightly different outcomes when applying the CCM/clustering approach on smoothed nominal versus standardised data for bigeye. Again, the most consistent results came when using the 3-year moving average time series, and we present results for the '3yr-nominal' and '3yr-standardised' analyses below.

3yr-nominal analysis - bigeye

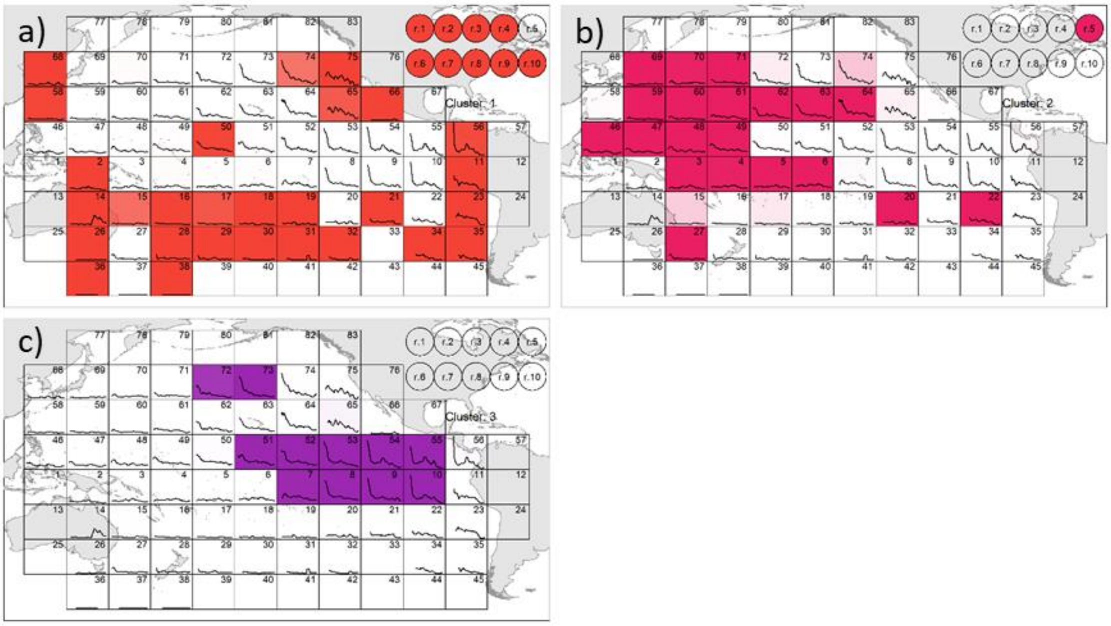

3yr-standardised analysis - bigeye

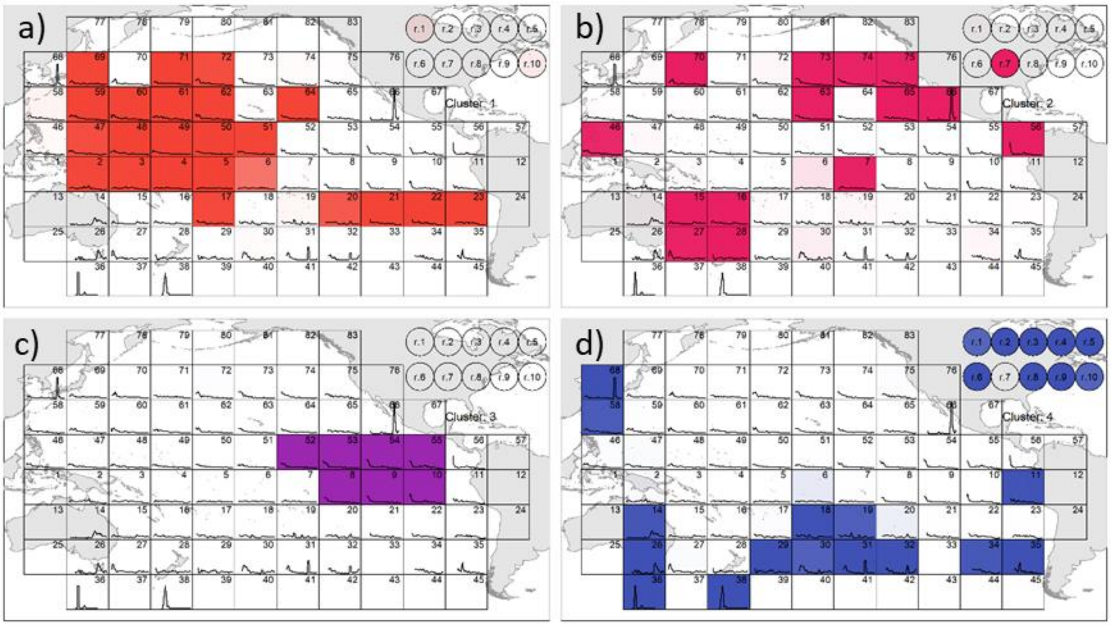

Figure 22 Results from the CCM/fuzzy clustering approach for the '3yr- nominal' (top panel) and '3yr-standardised' (bottom panel) analyses for bigeye. Black lines in each 15° × 15° grid cell are 3-year moving average CPUE time series for bigeye between 1950-2018 (note the different y-axis scale compared with Figure 21). Other information as for Figure 21. Note the allocation of colours to clusters is not comparable between the nominal and standardised figures. Within each cluster the lighter the shade indicates the lower the strength of the relationship between that cell and the other cells.

Three clusters were defined for the 3yr-nominal analysis and four clusters by the 3yr-standardised analysis (Figure 22). Most grid cells were assigned with high probability to the cluster they were classified to. There was some agreement in the patterns identified for nominal and standardised CPUE series, particularly regarding the location of the northwest Pacific [Figure 22 - cluster b) nominal and cluster a) standardised] and the equatorial eastern Pacific Ocean clusters [Figure 22 - cluster c) nominal and cluster c) standardised]. The main difference is that the 3yr-standardised analysis splits the cluster a) identified on the 3yr-nominal map in two clusters [i.e, Figure 22 – cluster a) nominal and clusters b) and d) standardised]. Note that in comparison to other clusters identified for bigeye, we have less confidence in how the larger cluster a) from the 3yr-nominal analysis and the two clusters b) and d) from the standardise analysis have arisen, as the cells within these clusters appear to share dynamics with r1-r10, the white noise time series. These clusters are less meaningful in terms of information for considering spatial structure of the stock assessment.

The results for bigeye provide support for one southern, an equatorial central-eastern Pacific region and equatorial-northwestern Pacific region within the WCPFC Convention Area. The CPUE analysis however, did not indicate a clear separation of an equatorial region from a northern region in the western and central Pacific, whereas the size composition analysis did indicate such a separation (Figure 16).

Synopsis and alternative spatial stratifications

The reviews and analyses included in this paper have the objective to provide an information base for considering spatial stratification of stock assessments of yellowfin and bigeye tuna in the WCPO. They, however, do not explicitly consider the data limitations and practical and technical challenges of the stock assessments or the jurisdictional and management structures that also have implications for spatial stratification of stock assessments. Reiterating the quote at the beginning of this paper by Cadrin et al., (2023) that ***"best scientific practices for defining spatial boundaries, spatial structure, and fleet structure in stock assessment should consider biological reality, theoretical assumptions, and practical solutions for meeting fishery management objectives"***, this synopsis attempts to make recommendations of alternative spatial stratifications that are both meaningful in terms of biological reality, practical in terms of data and implementation and useful for supporting the jurisdictional needs for management decision making, for further consideration.

Stratification of WCPO yellowfin and bigeye stock assessments can occur through either defining explicit spatial regions, grouping different flag/gear combinations that have similar characteristics of selectivity, CPUE and catch composition in a fleets-as-areas approach, or a combination of both. In relation to defining explicit spatial regions, the regional structure should initially be considered based on information on population structure from biological traits (genetics, growth, size at maturity etc.), spawning areas and timing, migration patterns and larval connectivity. This initial layer of information can then be overlaid by fishery information such as spatial distribution of catches or CPUE, CPUE trends and size distributions, and then the practical considerations related data availability, assessment model limitations and finally management/jurisdictional boundaries and needs.

An important example of when a tailored spatial stratification might be required to accommodate data and related assumptions is tag-recapture date. To use the tag-recapture data appropriately in a spatial model for either bigeye or yellowfin, tagged fish have to be assumed to have mixed with the untagged population so that their mortality is representative of the untagged population in the specific model region where they were released. In the assessment model a certain period is assumed after which tagged fish can be considered appropriately mixed for their recapture data to be considered representative of mortality rates of the untagged population. How quickly tagged fish mix can depend on various factors, and it is known that mixing times can vary depending on release areas. Therefore, spatial stratification in stock assessment models, notably the size of model strata, may need to be adapted for the incorporation of tag-recapture data.

Yellowfin tuna

At the scale of the Pacific Ocean most of the information discussed supports a level of independence of the yellowfin populations in the equatorial band from about 10-15°N to 10-15°S. This area encompasses the bulk of the yellowfin biomass and the majority of the spawning and juvenile recruitment. The population in this band has some connectivity with the those to the north and south, however the dynamics of the northern and southern regions would be expected to be influenced more by seasonal dynamics than the equatorial region, which was supported by the size composition and CPUE analyses. While the available tag data and genetics support some separation between the far eastern Pacific and far western Pacific populations, the tagging data do show movement across the boundaries of the assessment areas of the WCPFC and the IATTC, however it does not appear that strong mixing between the WCPFC and IATTC areas occurs. In the WCPO the regions of higher abundance and spawning areas are very much confined to the warm waters of the equatorial region, the seas around Indonesia and Philippines and South China Sea, the Kuroshio current from Philippines to southern Japan and the Coral Sea/East Australian Current region. The region in the north-east WCPO around Hawaii maybe however be somewhat isolated from the northwestern region of Pacific based on limited tag movement and low CPUE in the region between Japan and Hawaii. The different size composition in the northeast region suggests that the selectivity or growth of yellowfin might differ in that region, or that larger fish are more common in the size frequency in that area due to different exploitation levels. Unfortunately, the recent growth studies of yellowfin in the WCPO have not included samples from the Hawaiian region. Irrespective of the causes of different size composition of the catch, separate longline fleets for the northeast region and northwest region of the WCPO would seem appropriate, and spawning is also known to occur seasonally around the Hawaiian Islands and seamounts. For yellowfin there is support that a separate spatial stratum around Hawaii consistent with region 2 of the 9 region structure, is reasonable, either as a fleet-as-areas or a specific model region.

As to the region south of the Equatorial zone, there was no strong evidence for population structure from biological information or size composition, although the CPUE analysis did show clustering of cells in the southwestern Pacific, although the resolution is coarse.

In relation to the equatorial region the size composition analysis did not cover the Indonesia/Philippines/South China Sea region. While there is evidence that this region has connectivity with the broader western Pacific (tagging and genetics), it has quite different characteristics in relation to its archipelagic nature, its fisheries, and the high abundance and residency of very small yellowfin, along with larger adults which is possibly indicative of a degree of localised spawning and recruitment. Data availability and coverage is improving in this region under the WCPFC's West Pacific East Asia (WPEA) data improvement project. Our analysis supports a separate assessment region for the Indonesia/Philippines/Vietnam/South China Sea region, as has been included in recent assessments.

An important input data for the yellowfin assessment is tag-recapture data. The largest numbers of tagged yellowfin tuna have been released in the Bismarck and Solomon Seas and areas around the Solomon Islands and the Bismarck archipelago. These fish are known not to disperse as broadly or rapidly as those tagged on the open oceanic areas further west, and due to the high fishing pressure in this region few tags are recaptured after 1 year at liberty. The area has been allocated as a separate model region in previous assessments to allow a shorter mixing period assumption for the tag releases. This modelling consideration, and the observation that the populations in these archipelagic waters appear more resident supports retention of the current model region that encompasses the PNG/Solomon Islands area. Further, this area of archipelagic waters is treated differently under important WCPFC management measures and having a separate model region is therefore useful for management evaluations.

Tagging releases for yellowfin are mostly from locations east of 170°E or (referred to as Central Pacific cruises) and in the region around PNG/Solomon Islands. While most of the information suggest that there is no notable population structure of yellowfin in the central - western Pacific equatorial region of the WCPO, tag releases to the east of 170°E can take considerable time to move to the west meaning a larger equatorial region in the WCPO may be problematic for the tag mixing assumption. Few tag recaptures are reported after about one year at liberty in the equatorial region. To accommodate tagging data within the equatorial region may still require this area to be split as in the current 9 region model at 170°E.

There are also some yellowfin tagging data from the Coral Sea tagging programme in the mid-1990s included in past yellowfin assessments, however, these tagging data have unique features, discussed further below for bigeye that have necessitated a small model region be created off northeast Queensland coast (region 9, Figure 1f). Given the small number of yellowfin tagged in this program, the yellowfin peer review suggested that this region and the associated tags be removed in any simplification of the 9 region model structure.

Bigeye tuna

Similar to yellowfin, the information discussed supports a level of independence of the bigeye populations in the equatorial band from about 10-15°N to 10-15°S. However, there appears to be a more continuous population of bigeye in this latitudinal band across the entire Pacific Ocean and a significant amount of movement of bigeye is observed from the central western Pacific (WCPO area) to the eastern Pacific (EPO area). This connectivity has been noted before along with the suggestion that the bigeye stock in Pacific could be better assessed at the scale of the entire Pacific. However, a Pacific wide assessment is problematic due to different biological traits between the west and east Pacific most notably growth rates, and current integrated modelling software (MFCL or Stock Synthesis) do not allow spatially varying growth rates. While there is no clear separation between the WCPO and EPO stocks, an isolation by distance is proposed between the far western and far eastern Pacific and these regions are unlikely to have interrelated dynamics. A more appropriate structure might be a west Pacific, central Pacific and eastern Pacific region, however the central Pacific region would then be split between the WCPO and EPO.

Until a Pacific wide bigeye assessment is considered more feasible given the growth variation issues, we propose that a similar spatial stratification to that of yellowfin is appropriate, with equatorial, northern, southern, Indonesia/Philippines/Vietnam/South China Sea, and the Bismarck/Solomon's regions. However, we do note that additional considerations related to tagging data are necessary. The Coral Sea tagging data that are used in the WCPO bigeye assessments has unique features in that the tags were released in a localised seasonal spawning area, and the fishery that operates in that area has very high recapture rates that are not considered representative of a broader south Pacific region. This issue is dealt with in the bigeye assessment through creating a very small region off northeast Australia to encompass this tag release region. The other option is to remove these tagging data from the model altogether, but this tagging-programme has recaptures of fish at liberty for very long periods and provides information to the model on processes such as natural mortality, which can be influential, especially if natural mortality is estimated with the model (as is proposed in the 2023 assessment). As such retention of the small Coral Sea region is recommended if the Coral Sea tagging data are used.

The issue of mixing period assumptions for bigeye tag releases in the equatorial region is the same as for yellowfin, and splitting the equatorial region at 170°E, consistent with current practice, would seem appropriate.

Alternative spatial stratification

Figure *23* provides proposed alternative spatial stratification for the yellowfin and bigeye assessments in the WCPO. Ultimately, while much of the information would support a simpler 5 region model structure as proposed in Figure 23a, which simply collapses regions of the current 9 region model (Figure 1f), consideration of tag mixing assumptions requires additional complexity if tag data are used. The Coral Sea tag data necessitates the inclusion of a sixth region (**Figure *23***b, region 6) for bigeye, noting the Coral Sea tag data would be excluded for yellowfin. However, to utilise the central Pacific tag releases, a division of the equatorial region would be beneficial for better meeting tag mixing assumptions. Thus, resulting in a 6 region model (with a fleets-as-area separation of the northern region 1) for yellowfin (Figure 23c) and a 7 region model for bigeye (**Figure *23***d). While initially using a fleets-as-areas approach within the larger simplified regions is a practical approach for ease of transition between the 9 region structure and the simpler structures, fishery definitions could be revised to reduce the number of fisheries in the simpler spatial structures.

Referring back to the 9 region model structure, this structure is consistent with the information in this paper, and remains a reasonable option also. In fact, the separation of the northern and equatorial regions at 170°E is probably sensible based on the fisheries structures and tagging data considerations, and the indications that the Hawaiian yellowfin population is somewhat isolated from the equatorial and western Pacific populations. Similarly, separation of the southern region is consistent with separation of the large high seas fishery area to the east of New Zealand, which may be desirable for management reasons.

We suggest that exploring these simpler model stratifications to understand how they work with the available data and other model assumptions could begin in the current assessment with test models of the simplest options: the 5 region model for yellowfin (Figure 23 a), and the 6 region model for bigeye (Figure 23b). Despite the ambition of the SPC pre-assessment workshop (Hamer, 2023) to fully explore a range of simplified models in the 2023 assessment, this requires a substantial amount of time to be done properly if alternative spatial stratifications are to be proposed for management advice. We suggest this work really would need to be a stand-alone research project supported by and reviewed by the SC.

We invite the SC19:

- To consider the information in this paper and its implications for bigeye and yellowfin stock assessment spatial structure.
- Note that while simpler model structures are supported by the review, the information does not suggest that application of the current 9 region model is inappropriate.
- To consider whether to support a separate study to explore models of alternative spatial structure to better understand if simpler model structures might provide more optimal model performance and efficiency of stock assessments, and implications for other uses of the assessment models and outputs.

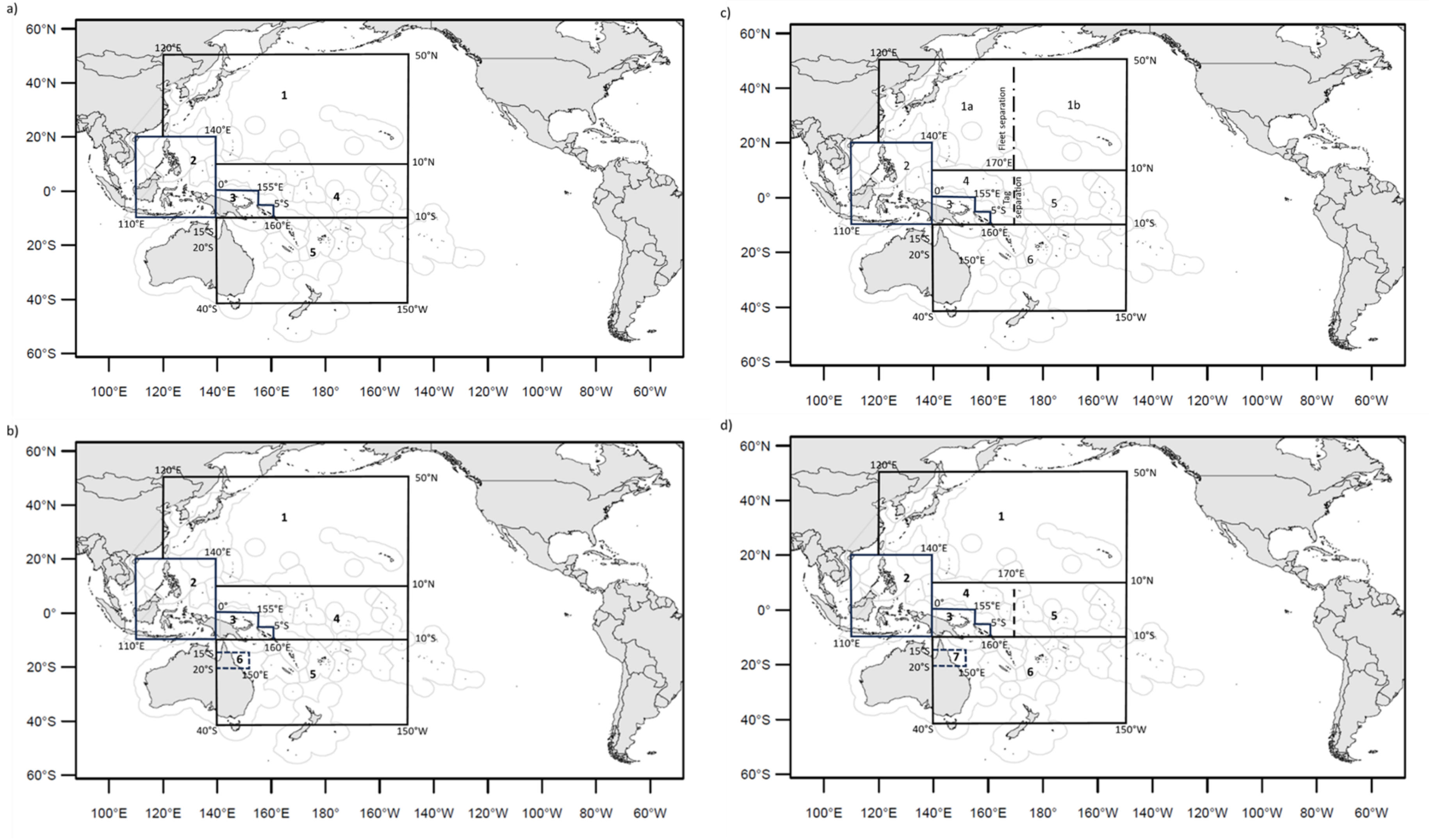

Figure 23 Maps showing options for spatial stratification of the WCPO yellowfin a) and c) and bigeye b) and d) assessments.

Acknowledgements

We would like to acknowledge the contribution of Nicholas Ducharme-Barth to the CPUE time series analysis work, Hirotaki Ijima and Marko Jusup from Japan FRA for providing permission to use their larval density maps, and David Itano from University of Hawaiʻi at Mānoa for his review and comments on this paper. The work was supported under the Scientific Services Provision contact between the WCPFC and The Pacific Community (SPC).

References

Aires-da-Silva, A.M., Maunder, M.N., Schaefer, K.M., Fuller, D.W., 2015. Improved growth estimates from integrated analysis of direct aging and tag-recapture data: An illustration with bigeye tuna (*Thunnus obesus*) of the eastern Pacific Ocean with implications for management. Fish. Res. 163, 119–126.

Anderson, G., Lal, M., Hampton, J., Smith, N., Rico, C., 2019. Close Kin Proximity in Yellowfin Tuna (*Thunnus albacares*) as a Driver of Population Genetic Structure in the Tropical Western and Central Pacific Ocean. Front. Mar. Sci. 6, 341. https://doi.org/10.3389/fmars.2019.00341

Appleyard, S.A., Grewe, P.M., Innes, B.H., Ward, R.D., 2001. Population structure of yellowfin tuna (*Thunnus albacares*) in the western Pacific Ocean, inferred from microsatellite loci. Mar. Biol. 139, 383–393. https://doi.org/10.1007/s002270100578

Boehlert, G., Mundy, B., 1994. Vertical and onshore-offshore distributional patterns of tuna larvae in relation to physical habitat features. Mar. Ecol. Prog. Ser. 107, 1–13. https://doi.org/10.3354/meps107001

Bonat, W.H. and Kokonendji, C.C. 2017. Flexible Tweedie regression models for continuous data. Journal of Statistical Computation and Simulation 87: 2138–2152.

Brooks, M., E., Kristensen, K., Benthem, K., J.,van, Magnusson, A., Berg, C., W., Nielsen, A., Skaug, H., J., Mächler, M., Bolker, B., M., 2017. glmmTMB Balances Speed and Flexibility Among Packages for Zero-inflated Generalized Linear Mixed Modeling. R J. 9, 378. https://doi.org/10.32614/RJ-2017-066

Buenafe, K.C.V., Everett, J.D., Dunn, D.C., Mercer, J., Suthers, I.M., Schilling, H.T., Hinchliffe, C., Dabalà, A., Richardson, A.J., 2022. A global, historical database of tuna, billfish, and saury larval distributions. Sci. Data 9, 423. https://doi.org/10.1038/s41597-022-01528-7

Cadrin, S.X., Goethel, D.R., Berger, A., Jardim, E., 2023. Best practices for defining spatial boundaries and spatial structure in stock assessment. Fish. Res. 262, 106650. https://doi.org/10.1016/j.fishres.2023.106650

Chang, C.-W., Ushio, M., Hsieh, C., 2017. Empirical dynamic modeling for beginners. Ecol. Res. 32, 785–796. https://doi.org/10.1007/s11284-017-1469-9

Chiang, H.-C., Hsu, C.-C., Lin, H.-D., Ma, G.C., Chiang, T.-Y., Yang, H.-Y., 2006. Population structure of bigeye tuna (*Thunnus obesus*) in the South China Sea, Philippine Sea and western Pacific Ocean inferred from mitochondrial DNA. Fish. Res. 79, 219–225. https://doi.org/10.1016/j.fishres.2005.11.026

Davies, N., Harley, S., Hampton, J., McKechnie, S., 2014. Stock assessment of yellowfin tuna in the Western and Central Pacific Ocean. WCPFC-SC10-2014/SA-WP-04..

Deyle, E.R., Fogarty, M., Hsieh, C., Kaufman, L., MacCall, A.D., Munch, S.B., Perretti, C.T., Ye, H., Sugihara, G., 2013. Predicting climate effects on Pacific sardine. Proc. Natl. Acad. Sci. 110, 6430–6435. https://doi.org/10.1073/pnas.1215506110

Deyle, E.R., Sugihara, G., 2011. Generalized Theorems for Nonlinear State Space Reconstruction. PLoS ONE 6, e18295. https://doi.org/10.1371/journal.pone.0018295

Ducharme-Barth, Nicholas, Vincent, M., Hampton, J., Hamer, P., Williams, P., Pilling, G., 2020. Stock assessment of bigeye tuna in the western and central Pacific Ocean. WCPFC-SC16-2020/SA-WP-03 [REV3].

Ducharme-Barth, N, Vincent, M., Vidal, T., Hamer, P., 2020. Analysis of Pacific-wide operational longline dataset for bigeye and yellowfin tuna catch-per-unit-effort (CPUE). WCPFC-SC16-2020/SA- IP-07.

Evans, K., Grewe, P.M., Foster, S.D., Gosselin, T., Gunasekera, R.M., Lansdell, M.J., 2019. Connectivity of tuna and billfish species targeted by the Australian Eastern Tuna and Billfish Fishery with the broader Western Pacific Ocean. WCPFC-SC15-2019/SA-IP13.

Evans, K., Patterson, T., Pedersen, M., 2011. Movement patterns of yellowfin tuna in the Coral Sea region: defining connectivity with stocks in the western Pacific Ocean region. Final Report to the Australian Fisheries Management Authority. CSIRO Marine and Atmospheric Research, Hobart, TAS, Australia.

Farley, J., Eveson, P., Krusic-Golub, K., Chang, S.K., 2017. Age, growth and maturity of bigeye tuna in the Pacific. WCPFC-SC13-2017/SA-WP-XX). Rarotonga, Cook Islands, 9–17 August 2017.

Farley, J., Eveson, P., Krusic-Golub, K., Clear, N., Sanchez, C., Roupsard, F., Satoh, K., 2018. Update on age and growth of bigeye tuna in the WCPO. WCPFC Project 81. Working Paper WCPFC-SC14-2018/SA-WP-01.

Farley, J., Krusic-Golub, K., Eveson, P., Clear, N., Rouspard, F., Sanchez, C., Nicol, S., Hampton, J., 2020. Age and growth of yellowfin and bigeye tuna in the western and central Pacific Ocean from otoliths. WCPFC-SC16-2020/SA- WP- 02.

Glaser, S.M., Ye, H., Maunder, M., MacCall, A., Fogarty, M., Sugihara, G., 2011. Detecting and forecasting complex nonlinear dynamics in spatially structured catch-per-unit-effort time series for North Pacific albacore (*Thunnus alalunga*). Can. J. Fish. Aquat. Sci. 68, 400–412. https://doi.org/10.1139/f10-160

Glaser, S.M., Ye, H., Sugihara, G., 2014. A nonlinear, low data requirement model for producing spatially explicit fishery forecasts. Fish. Oceanogr. 23, 45–53. https://doi.org/10.1111/fog.12042

Grewe, P.M., Feutry, P., Hill, P.L., Gunasekera, R.M., Schaefer, K.M., Itano, D.G., Fuller, D.W., Foster, S.D., Davies, C.R., 2015. Evidence of discrete yellowfin tuna (*Thunnus albacares*) populations demands rethink of management for this globally important resource. Sci Rep 5, 16916. https://doi.org/10.1038/srep16916

Grewe, P.M., Hampton, J., 1998. An assessment of bigeye (*Thunnus obesus*) population structure in the Pacific Ocean based on mitochondrial DNA and DNA microsatellite analysis. JIMAR Contribution 98-330.

Grewe, P.M., Wudianto, C.H., Proctor, C.H., Adam, M.S., Jauhary, A.R., Schaefer, K., Itano, D.G., Evans, K., Killian, A., Foster, S.D., Gosselin, T., Feutry, P., Aulich, J., Gunasekera, R.M., Lansdell, M., Davies, C.R., 2019. Population Structure and Connectivity of Tropical Tuna Species across the Indo Pacific Ocean Region. WCPFC-SC15-2019/SA-IP-15.

Gunn, J.S., Clear, N.P., Ward, R.D., Appleyard, S.A., Grewe, P.M., Innes, B.H., 2002. The origin of recruits to the east coast yellowfin tuna fishery and the delineation of the structure of yellowfin stocks in the western Pacific. Final Report to the Fisheries Research and Development Corporation. CSIRO Marine Research, Hobart, TAS, Australia.

Hamer, P., 2023. Report from the SPC Pre-assessment Workshop – April 2023. WCPFC-SC19-2023/ SA-IP- 01.

Hampton, J., Fournier, D.A., 2001. A spatially-disaggregated, length-based, age-structured population model of yellowfin tuna (*Thunnus albacares*) in the western and central Pacific Ocean. Mar. Freshw. Res. 52, 937–963.

Hampton, J., Bigelow, K. and Labelle, M. 1998. Effect of longline fishing depth, water temperature and dissolved oxygen on bigeye tuna (*Thunnus obesus*) abundance indices. Technical report, Oceanic Fisheries Programme, Secretariat of the Pacific Community (SPC).

Hampton, J., Gunn, J.S., 1998. Exploitation and movements of yellowfin tuna (*Thunnus albacares*) and bigeye tuna (*T. obesus*) tagged in the north-western Coral Sea. Mar. Freshw. Res. 49, 475–489.

Hampton, J., Kleiber, P., 2003. Stock assessment of yellowfin tuna in the western and central Pacific Ocean. WP YFT-1, SCTB 16, Mooloolaba, Australia, 9–16 July 2003.

Hampton, J., Kleiber, P., Langley, A., Hiramatsu, K., 2004a. Stock assessment of yellowfin tuna in the western and central Pacific Ocean. WP SA-1, SCTB 17, Majuro, Republic of Marshall Islands, 9−18 August 2004.

Hampton, J., Kleiber, P., Langley, A., Hiramatsu, K., 2004b. Stock assessment of bigeye tuna in the western and central Pacific Ocean. Working Paper SA-2, SCTB 17, Majuro, Marshall Islands.

Hampton, J., Kleiber, P., Langley, A., Takeuchi, Y., Ichinokawa, M., 2005. Stock assessment of bigeye tuna in the western and central Pacific Ocean. WCPFC-SC1-2005/SA-WP-02.

Hampton, J, Kleiber, P., Langley, A., Takeuchi, Y., Ichinokawa, M., 2005. Stock assessment of yellowfin tuna in the western and central Pacific Ocean. WCPFC-SC1-2005/SA-WP-1.

Hampton, J., Kleiber, P., Takeuchi, Y., Kurota, H., Maunder, M., 2003. Stock assessment of bigeye tuna in the western and central Pacific Ocean, with comparisons to the entire Pacific Ocean. WP BET-1, SCTB 16, Mooloolaba, Australia, 9−16 July 2003.

Hampton, J., Langley, A., Kleiber, P., 2006a. Stock assessment of yellowfin tuna in the western and central Pacific Ocean, including an analysis of management options. WCPFC-SC2-2006/ SA-WP-01.

Hampton, J., Langley, A., Kleiber, P., 2006b. Stock assessment of bigeye tuna in the western and central Pacific Ocean, including an analysis of management options. WCPFC-SC2-2006/SA-WP-02.

Hampton, J., Maunder, M., 2006. An update of Pacific-wide assessment of bigeye tuna with comparisons with eastern Pacific assessment results. Document SAR-7-07c.ii. IATTC Working Group to Review Stock Assessments, 7th meeting, La Jolla, California (USA), 15-19 May 2006.

Hampton, J., Maunder, M., 2005. Comparison of Pacific-wide, western and central Pacific, and eastern Pacific assessments of bigeye tuna. 1st Meeting of the Scientific Committee of the Western and Central Pacific Fisheries Commission WCPFC–SC1 Noumea, New Caledonia 8–19 August 2005).

Hampton, J., Williams, P., 2005. A description of tag-recapture data for bigeye tuna in the western and central Pacific Ocean. Col Vol Sci Pap ICCAT 57, 85–93.

Harley, S.J., Davies, N., Hampton, J., McKechnie, S., 2014. Stock assessment of bigeye tuna in the Western and Central Pacific Ocean. WCPFC-SC10-2014/SA-WP-01.

Hartig, F. 2022. DHARMa: Residual Diagnostics for Hierarchical (Multi-Level / Mixed) Regression Models. R package version 0.4.5.

Hoyle, S., Nicol, S., Itano, D., 2009. Revised biological parameter estimates for application in yellowfin stock assessment. WCPFC-SC5-2009/BI-WP-3 Rev).

Ianelli, J., Maunder, M.N., Punt, Andre.E., 2012. Independent review of the 2011 WCPO bigeye tuna assessment. WCPFC-SC8-2012/SA-WP-01.

Ijima, H., Jusup, M., 2023. Tuna and billfish larval distributions in a warming ocean. https://doi.org/10.48550/arXiv.2304.09442

Itano, D., 2000. The reproductive biology of yellowfin tuna (*Thunnus albacares*) in Hawaiian waters and the western tropical Pacific Ocean: Project summary (JIMAR Contribution 00-328 No. SOEST 00-01).

Itano, D.G., Holland, K.N., 2000. Displacement and vulnerability of bigeye tuna (*Thunnus obesus*) and yellowfin tuna (*Thunnus albacares*) in relation to FADs and natural aggregation points. Aquatic Liv. Res. 13 (4), 213-223. https://doi.org/10.1016/S0990-7440(00)01062-7

Jorgensen, B. 1997. The theory of dispersion models. CRC Press.

Lam, C.H., Tam, C., Kobayashi, D.R., Lutcavage, M.E., 2020. Complex Dispersal of Adult Yellowfin Tuna from the Main Hawaiian Islands. Front. Mar. Sci. 7, 138. https://doi.org/10.3389/fmars.2020.00138

Langley, A., Hoyle, S.D., Hampton, J., 2011. Stock assessment of yellowfin tuna in the Western and Central Pacific Ocean. WCPFC-SC7-2011/SA-WP-03

Lehodey, P., Senina, I., Calmettes, B., Dessert, M., Nicol, S., Hampton, J., Smith, N., Gorgues, T., Aumont, O., Lengaigne, M., Menkes, C., Gehlen, M., 2017. Modelling the impact of climate change including ocean acidification on Pacific yellowfin tuna. Western and Central Pacific Fisheries

Commission Scientific Committee, Western and Central Pacific Fisheries Commission Scientific Committee, Working Paper WCPFC- SC13-2017/EB-WP-01.

Lehodey, P., Senina, I., Murtugudde, R., 2008. A spatial ecosystem and populations dynamics model (SEAPODYM) – Modeling of tuna and tuna-like populations. Prog. Oceanogr. 78, 304–318. https://doi.org/10.1016/j.pocean.2008.06.004

Lennert-Cody, C.E., Maunder, M.N., Aires-da-Silva, A., Minami, M., 2013. Defining population spatial units: Simultaneous analysis of frequency distributions and time series. Fish. Res. 139, 85–92. https://doi.org/10.1016/j.fishres.2012.10.001

Lennert-Cody, C.E., Minami, M., Tomlinson, P.K., Maunder, M.N., 2010. Exploratory analysis of spatial–temporal patterns in length–frequency data: An example of distributional regression trees. Fish. Res. 102, 323–326. https://doi.org/10.1016/j.fishres.2009.11.014

Leroy, B., Evans, K., Scutt Phillips, J., Patterson, T., Caillot, S., Usu, T., Kumasi, B., Davies, C., Nicol, S., Kumoru, L., 2014. Progress report on archical tagging within the Papua New Guinea Tagging Program. WCFPC-SC10-2014/RP-PTTP-05.

Maechlaer, M., Rousseeuw, P., Struyf, A., Hubert, M., Hornik, K., 2022. cluster: Cluster Analysis Basics and Extensions.

McKechnie, S., Pilling, G., Hampton, J., 2017. Stock assessment of bigeye tuna in the western and central Pacific Ocean. WCPFC-SC13-2017/SA-WP-05.

Moore, B.R., Bell, J.D., Evans, K., Farley, J., Grewe, P.M., Hampton, J., Marie, A.D., Minte-Vera, C., Nicol, S., Pilling, G.M., Scutt Phillips, J., Tremblay-Boyer, L., Williams, A.J., Smith, N., 2020. Defining the stock structures of key commercial tunas in the Pacific Ocean I: Current knowledge and main uncertainties. Fish. Res. 230, 105525. https://doi.org/10.1016/j.fishres.2020.105525

Moore, B.R., Lestari, P., Cutmore, S.C., Proctor, C., Lester, R.J.G., 2019. Movement of juvenile tuna deduced from parasite data. ICES J. Mar. Sci. 76, 1678–1689. https://doi.org/10.1093/icesjms/fsz022

Muhling, B.A., Lamkin, J.T., Alemany, F., García, A., Farley, J., Ingram, G.W., Berastegui, D.A., Reglero, P., Carrion, R.L., 2017. Reproduction and larval biology in tunas, and the importance of restricted area spawning grounds. Rev. Fish Biol. Fish. 27, 697–732. https://doi.org/10.1007/s11160-017-9471-4

Munch, S.B., Brias, A., Sugihara, G., Rogers, T.L., 2020. Frequently asked questions about nonlinear dynamics and empirical dynamic modelling. ICES J. Mar. Sci. 77, 1463–1479. https://doi.org/10.1093/icesjms/fsz209

Munch, S.B., Giron-Nava, A., Sugihara, G., 2018. Nonlinear dynamics and noise in fisheries recruitment: A global meta-analysis. Fish Fish. 19, 964–973. https://doi.org/10.1111/faf.12304

Natasha, J., Stockwell, B.L., Marie, A.D., Hampton, J., Smith, N., Nicol, S., Rico, C., 2022. No Population Structure of Bigeye Tunas (*Thunnus obesus*) in the Western and Central Pacific Ocean Indicated by Single Nucleotide Polymorphisms. Front. Mar. Sci. 9, 799684. https://doi.org/10.3389/fmars.2022.799684

Nepomuceno, L.T., Bacordo, R.S., Camu, D.G.Y., Ramiscal, R.V., 2020. Abundance, Distribution, and Diversity of Tuna Larvae (Family Scombridae) in the Philippine waters. Philipp. J. Fish. 231–237. https://doi.org/10.31398/tpjf/27.2.2019-0010

Nicol, S., Lehodey, P., Senina, I., Bromhead, D., Frommel, A.Y., Hampton, J., Havenhand, J., Margulies, D., Munday, P.L., Scholey, V., Williamson, J.E., Smith, N., 2022. Ocean Futures for the World's Largest Yellowfin Tuna Population Under the Combined Effects of Ocean Warming and Acidification. Front. Mar. Sci. 9, 816772. https://doi.org/10.3389/fmars.2022.816772

Nikaido, H., N. Miyabe, and S. Ueyanagi. 1991. Spawning time and frequency of bigeye tuna, *Thunnus obesus*. Nat. Res. Inst. Far. Seas Fish., Bull., 28:47-73.

Nishikawa, Y., Honma, M., Ueyanagi, S., Kikawa, S., 1985. Average distribution of larvae of oceanic species of scombroid fishes, 1956–1981. Far Seas FishResLab 99 P.

Pecoraro, C., Babbucci, M., Franch, R., Rico, C., Papetti, C., Chassot, E., Bodin, N., Cariani, A., Bargelloni, L., Tinti, F., 2018. The population genomics of yellowfin tuna (*Thunnus albacares*) at global geographic scale challenges current stock delineation. Sci. Rep. 8, 13890. https://doi.org/10.1038/s41598-018-32331-3

Proctor, C.H., Lester, R.G.J., Clear, N.P., Grewe, P.M., Moore, B.R., Eveson, J.P., Lestari, P., Wudji, A., Taufik, M., Wudianto, Lansdell, M.J., Hill, P.L., Dietz, C., Thompson, J.M., Cutmore, S.C., Foster, S.D., Gosselin, T., Davies, C.R., 2019. Population structure of yellowfin tuna (*Thunnus albacares*) and bigeye tuna (*T. obesus*) in the Indonesian region. Final Report as output of ACIAR Project FIS/2009/059. Australian Centre for International Agricultural Research, Canberra.

Punt, A.E., Maunder, M.N., Ianelli, J., 2023. Independent review of recent WCPO yellowfin tuna assessment. WCPFC-SC19-2023/SA- WP- 01.

R Core Team, 2021. R: A Language and Environment for Statistical Computing.

Reglero, P., Tittensor, D., Álvarez-Berastegui, D., Aparicio-González, A., Worm, B., 2014. Worldwide distributions of tuna larvae: revisiting hypotheses on environmental requirements for spawning habitats. Mar. Ecol. Prog. Ser. 501, 207–224. https://doi.org/10.3354/meps10666

Rooker, J.R., David Wells, R.J., Itano, D.G., Thorrold, S.R., Lee, J.M., 2016. Natal origin and population connectivity of bigeye and yellowfin tuna in the Pacific Ocean. Fish. Oceanogr. 25, 277–291. https://doi.org/10.1111/fog.12154

Satoh, K., Katayama, S., Tanabe, T., Okamoto, K., 2023. Connectivity in juvenile yellowfin tuna Thunnus albacares between temperate and tropical regions of the western Pacific Ocean. Mar. Ecol. Prog. Ser. 713, 151–172. https://doi.org/10.3354/meps14325

Schaefer, K., Fuller, D., 2023. Spatiotemporal variability in the reproductive biology of yellowfin tuna (*Thunnus albacares*) in the eastern Pacific Ocean. Fish. Res. 284 (4), 106225, https://doi.org/10.1016/j.fishres.2022.106225

Schaefer, K., Fuller, D., 2009. Horizontal movements of bigeye tuna (Thunnus obesus) in the eastern Pacific Ocean as determined from conventional and archival tagging experiment initiated during 2000-2005. Inter-American Tropical Tuna Commission Bulletin 24, 191–247.

Schaefer, K., Fuller, D., Hampton, J., Caillot, S., Leroy, B., Itano, D., 2015. Movements, dispersion, and mixing of bigeye tuna (*Thunnus obesus*) tagged and released in the equatorial Central Pacific Ocean, with conventional and archival tags. Fish. Res. 161, 336–355.

Schaefer, K.M., 1998. Reproductive biology of yellowfin tuna (*Thunnus albacares*) in the eastern Pacific Ocean (No. 21: 205–272.). IATTC Bulletin.

Schaefer, K.M., 1991. Geographic variation in morphometric characters and gill-Raker counts of yellowfin tuna *Thunnus albacares* from the Pacific Ocean. Fishery Bulletin, U.S. 89:289-297.

Schaefer, K.M., Fuller, D.W., Miyabe, N., 2005. Reproductive biology of bigeye tuna (*Thunnus obesus*) in the eastern and central Pacific Ocean. No. 23(1). 35p.). IATTC Bulletin.

Senina, I., Briand, G., Lehodey, P., Nicol, S., Hampton, J., Williams, P., 2021. Reference model of bigeye tuna using SEAPODYM with catch, length and conventional tagging data (Pohnpei: Western and Central Pacific Fisheries Commission). WCPFC-SC17-2021/EB-IP-08.

Senina, I., Hampton, J., Bonin, L., Lehodey, P., Hamer, P., Nicol, S., 2023. Spatial structure and regional connectivity of bigeye and yellowfin tuna stocks in the WCPO derived from the reference SEAPODYM models, WCPFC-SC19-2023/SA-IP-06.

Senina, I., Lehodey, P., Calmettes, B., Dessert, M., Hampton, J., Smith, N., Gorgues, T., Aumont, O., Lengaigne, M., Nicol, S., Gehlen, M., 2018. Impact of climate change on tropical Pacific tuna and their fisheries in Pacific Islands waters and high seas areas. WCPFC-SC14-2018/EB-WP-01.

Senina, I., Lehodey, P., Calmettes, B., Nicol, S., Caillot, S., Hampton, J., Williams, P., 2015. SEAPODYM Application for Yellowfin Tuna in the Pacific Ocean. WCPFC-SC11-2015/EB- IP- 01.

Senina, I., Lehodey, P., Sibert, J., Hampton, J., 2020. Integrating tagging and fisheries data into a spatial population dynamics model to improve its predictive skills. Can. J. Fish. Aquat. Sci. 77, 576–593. https://doi.org/10.1139/cjfas-2018-0470

Sugihara, G., May, R., Ye, H., Hsieh, C.H., Deyle, E., Fogarty, M., Munch, S., 2012. Detecting Causality in Complex Ecosystems. Science 338, 496–500. https://doi.org/10.1126/science.1227079

Suzuki, Z., Tomlinson, P.K., Honma, M., 1978. Population structure of Pacific yellowfin tuna. Inter-Am. Trop. Tuna Comm. Bull. 17, 1–358.

Takens, F., 1981. Detecting strange attractors in turbulence. Lect. Notes Math. 898, 16.

Teears, T., Peatman, T., Williams, P., Scutt Phillips, J., Magnusson, A., Day, J., Hampton, J., McKechnie, S., Hamer, P., 2023. CPUE analysis and data inputs for the 2023 bigeye and yellowfin tuna assessments in the WCPO. WCPFC-SC19-2023/SC19- SA- WP- 03.

Tremblay-Boyer, L., McKechnie, S., Pilling, G., Hampton, J., 2017. Stock assessment of yellowfin tuna in the Western and Central Pacific Ocean. WCPFC-SC13-2017/SA-WP-06).

Tsonis, A.A., Deyle, E.R., Ye, H., Sugihara, G., 2018. Convergent Cross Mapping: Theory and an Example, in: Tsonis, A.A. (Ed.), Advances in Nonlinear Geosciences. Springer International Publishing, Cham, pp. 587–600. https://doi.org/10.1007/978-3-319-58895-7_27

Vincent, M., Ducharme-Barth, N., 2020. Background analyses for the 2020 stock assessments of bigeye and yellowfin tuna in the western and central Pacific Ocean. WCPFC-SC16-2020/SA- IP- 06.

Vincent, M., Ducharme-Barth, N., Hamer, P., Hampton, J., Williams, P., Pilling, G., 2020. Stock assessment of yellowfin tuna in the western and central Pacific Ocean. WCPFC-SC16-2020/SA-WP-04-Rev2.

Wells, R., Rooker, J., Itano, D., 2012. Nursery origin of yellowfin tuna in the Hawaiian Islands. Mar. Ecol. Prog. Ser. 461, 187–196. https://doi.org/10.3354/meps09833

Wu, Z., Xu, Q., Zhu, J., Dai, X., Xu, L., 2014. Genetic population structure of the bigeye tuna *Thunnus obesus* in the central Pacific Ocean based on mtDNA Cytb sequences. Fish. Sci. 80, 415–426. https://doi.org/10.1007/s12562-014-0712-3

Xu, H., Lennart-Cody, C., 2023. FishFreqTree: IATTC's regression tree R package for fisheries' size frequency data.

Ye, H., Clark, A., Deyle, E., Munch, S., 2019. rEDM: Applications of Empirical Dynamic Modeling from Time Series.

Zuur, A. Ieno, E.N., Walker, N.J., Saveliev, A.A. and Smith, G.M. 2009. Mixed effects models and extensions in ecology with R. Springer.

Appendices

Appendix 1 – Biological information review

Summaries of information from various biological and other sources with implications for considering model spatial stratifications.

a) Yellowfin tuna

Information source	**Summary**	**Support for spatial population structure in WCPO**	**References**
Spawning areas and larval distribution	Information from reproductive studies and larval sampling of yellowfin tuna show a broad continuous spawning region across tropical waters of the WCPO, including the waters around Indonesia and the Philippines. Spawning occurs all year in the tropics, also observed for the EPO, but is seasonal and less expansive in the sub-tropical waters from the south of Japan across to Hawaii, where spawning occurs seasonally in water temps >24°C, i.e., April-September (northern spring-summer) but noting that spawning shuts down around Hawaii when SST begins to decline in the fall, despite the SST remaining typically above 24°C all year. Seasonal spawning peaks also appear to occur around Philippines, despite SST being consistently above 24°C. Spawning has been observed in the Coral Sea northeast Australia, to the south of PNG and the Solomon Islands where it is also seasonal and more prevalent in warmer months from October to March (southern spring –summer). The historical larval data sets from Japanese sampling programs show general higher larval densities in a broad region of the western Pacific from the Philippines down to PNG and Solomons. However, consistent with spawning observations, larvae can occur throughout the entire equatorial region of the central and western Pacific. There is, however, evidence of a break in the continuity of the equatorial larval distribution at around 140°W, and separate larval areas in the eastern Pacific Ocean (EPO) that would suggest separate spawning areas in the EPO. See **Figure 2**	**YES:** Support for sperate spawning areas in the EPO. All year spawning in the WCPO tropical region suggests the spawning biomass in the tropics is disproportionately more important for stock replenishment than in sub-tropical regions. Seasonal spawning in the regions north and south of the equatorial region maybe be related to seasonal movements of some fish away from the equatorial regions, but around the Hawaiian region it appears this may not be the case and that seasonal spawning occurs for resident fish as temperature drops in the fall (autumn). The patterns of larval distribution and spawning support stratification of the tropical region and north and south and sub-tropical/temperate regions.	(Boehlert and Mundy, 1994; Buenafe et al., 2022; Ijima and Jusup, 2023; Itano, 2000; Muhling et al., 2017; Nepomuceno et al., 2020; Nishikawa et al., 1985; Reglero et al., 2014; Schaefer, 1998; Schaefer and Fuller, 2022; Suzuki et al., 1978)
Small juveniles (< 40 cm FL)	Small juveniles, at least 30 cm FL, are caught in purse seine and pole and line fisheries throughout the equatorial WCPO and from Philippines/Indonesia to south of Japan. Port sampling indicates very high catches of small juveniles in archipelagic waters and seas around Indonesia/Philippines/Vietnam. Other studies have sampled small juveniles around Solomon Islands, Marshall and Line Is, and Hawaii, indicating they are	**YES:** Stratification of the Indonesia/Philippines region may be supported due to a combination of fishery selectivity, gears and high abundance of small juveniles.	(Rooker et al., 2016; Vincent et al., 2020)

	widespread, consistent with the widespread larval distribution, and suggest that there are no clearly defined juvenile nursery areas.		
Growth rates and maximum size	Spatial growth comparisons have suggested the possibility of some geographic variation in yellowfin growth in the WCPO but the data/comparison are inconclusive due to differences in sample numbers between areas and across different parts of the growth curve. Comparing studies in the WCPO and EPO also suffers from methodological differences in the preparation and ageing methods. Other studies based on growth estimated from length modes within MFCL models suggested slower growth in Indonesia/Philippines compared to the broader WCPO.	**No:** Comparisons are not sufficiently conclusive for indicating population structure based on growth variation within the WCPO. Spatial growth variation cannot be accommodated in the MFCL age-structured model and is better dealt with by a length and age structured model.	(Farley et al., 2020; Hoyle et al., 2009)
Morphometric, meristics, and size at maturity	Various early studies (1940s-1960s) reported morphometric differences among areas of the Pacific and a potential cline in morphometric features along the equator that supported difference between the EPO and WCPO regions. More recent morphometric and meristic analyses of samples in the late 1980's further showed difference among samples from the EPO and WCPO regions, including between Hawaii, Japan and Australia. There are, also indications that size at 50% maturity differs between WCPO and EPO and also between Indonesia/Philippines and the western equatorial Pacific and Hawaii.	**Yes:** different sizes at 50% maturity for the Indonesia/Philippines region, along with possible growth variation previously suggested, lend further support for a degree of isolation for this region. Similarly, different morphometrics and meristics for Hawaiian samples supports other information that indicates the population around Hawaii is likely a sub-population within the WCPO stock.	(Itano, 2000; Moore et al., 2020; Schaefer, 1998; Schaefer, 1991)
Genetics	Pacific wide genetic studies indicate reproductively isolated populations in the far eastern Pacific and the central and western Pacific. Variation within the WCPO is less clear with different studies applying different markers, and some with low sample sizes and low statistical power, and no single studies cover both latitudinal and longitudinal variation. Evidence for genetic structure in the WCPO from more recent studies using SNPs is also variable. One study found differences between the EPO (Baja), central Pacific (Tokelau) and the western Pacific (Coral Sea), another found differences between EPO (Mexico) and WCPO (Nauru and Solomon Is), but another study focussed solely on the WCPO did not find differences between samples from Australia, Fiji and the Marshall Is. Studies in Indonesia suggested a genetic cline with samples from more easterly locations being more similar to samples from the WCPO than the Indian Ocean.	**No:** no consistent, temporally replicated conclusive evidence for genetic sub-populations in the WCPO. Good evidence to support solation by distance between WCPO and EPO, consistent with other information herein.	(Anderson et al., 2019; Appleyard et al., 2001; Evans et al., 2019; Grewe et al., 2019, 2015; Pecoraro et al., 2018; Proctor et al., 2019)

Otolith chemistry	Otolith chemistry studies have explored connectivity between small (young-of-year 30-40 cm) juveniles and sub-adults (1-2+ years of age, 70-110 cm) of the same cohorts within the WCPO. While the young of year samples had reasonable spatial coverage to generate the baseline (origin) groups, the sub-adults had low spatial coverage, constrained to two areas of interest, Hawaii and Marshall Is. None the less, sub-adults from Hawaii and Marshall Islands appeared mostly derived from young-of- year from those same areas. Another study sampled otoliths from young of year in the Banda Sea in Indonesia, the southern Philippines, northeast Solomon Islands, Fiji, and the northwest Coral See and then compared the otolith chemistry of the young of year to the core region of otoliths from two and three year old fish caught off the east coast of NSW and southern Qld in the Tasman Sea. The results suggested that majority of the older samples appeared to originate from the Coral Sea. Similar to the genetics information, otolith chemistry of samples from around Indonesia, indicated that the juvenile fish that were sampled there had likely originated and remained in the area around Indonesia. The most recent otolith chemistry study provided good evidence that the majority of small (~30-40 cm) juvenile yellowfin captured around Japan originated from very small juveniles (< 10cm) sampled further south in the western Pacific tropical region. This suggests dispersal/movement from the equatorial western Pacific spawning areas via the western boundary current (Kuroshio) was most important for juvenile recruitment around Japan.	**Maybe:** information is not sufficient at the WCPO scale and further appropriately designed studies are required to enable broader spatial comparisons, and including adult life stages. Support for limited large-scale movements of juveniles, and evidence for juvenile residency in the Indonesian area.	(Gunn et al., 2002; Rooker et al., 2016; Satoh et al., 2023; Wells et al., 2012)
Parasites	Limited work, comparisons between juveniles sampled in the Indonesian area and adjacent Indian Ocean and western Pacific suggested limited mixing, study did not sample adults.	**Maybe:** insufficient spatial sampling throughout WCPO, but support for residency and separation of small juveniles in the Indonesia region from the broader WCPO.	(Moore et al., 2019; Proctor et al., 2019)
Tagging	Various tag programmes in the WCPO and EPO have occurred over several decades. In the WCPO since 1989 approximately 170,000 tagged yellowfin have been released, with over 25,000 recaptures. Most releases were <80 cm FL and therefore are considered sub-adults, also most were released in the western and central equatorial region, in particular the Bismarck and Solomons Seas. Smaller numbers have been released south of Japan, and around Hawaii, and in the Coral Sea. Tag-recapture summaries are presented in most recent stock assessments (see Figure 3). Most recaptures of WCPO released fish have been within the WCPO region but numerous have also been in the western area of the EPO, particular for fish released in the central WCPO. EPO tagged fish off Central America have rarely been recaptured in the central and western Pacific. Most recaptures of equatorial tagged fish have involved	**Yes:** most tag recaptures of equatorial released fish are in the equatorial regions. The PNG/Solomons/Bismarck Sea releases general mix less with the broader equatorial region suggesting higher residency in that region, at least for the sub-adult/juvenile fish. Supports stratification of the equatorial region and also the PNG/Solomons/Bismarck region.	(Nicholas Ducharme-Barth et al., 2020; Evans et al., 2011; Itano and Holland, 2000, Lam et al., 2020; Langley et al., 2011; Moore et al., 2020; Vincent et al., 2020; Vincent and Ducharme-Barth, 2020).

	longitudinal rather than latitudinal displacements. Although movements between southern Japan, Hawaii and the equatorial regions are observed. Fish tagged around the PNG, Solomons/Bismarck Sea area show particularly low movement out of the that region. Archival tag movements were generally consistent with traditional tags. Limited studies with satellite tags have occurred in the WCPO, with releases off Australia (Tasman/Coral Sea) and Hawaii. The study in Australia released 20 larger adults with PSATs, and measured movements up to 1500 km, with the longest time tracked at 168 days. Studies around Hawaii had only short maximum liberty times of 59 days but showed variable movement behaviours, some moved over 800 km. The results show scope for long distance movement of adults. See **Figure 3**		
CPUE spatial	Spatial patterns in longline CPUE have been produced for the entire Pacific Ocean for yellowfin and are typically included in recent yellowfin assessments. They show clear and consistent spatial patterns, with higher nominal CPUE in the equatorial regions between 10°N and 10°S. In recent decades the areas of higher CPUE have contracted to the equatorial region west of 180°E. The CPUE patterns also indicate that higher abundances also occur further to the north and south of the western Pacific equatorial region compared to the central Pacific equatorial region where CPUE reduces greatly to the east from 150°W. The higher CPUE north and south of the equator in the western Pacific appears associated with warmer waters of the western boundary currents such as the East Australian Current and the Kuroshio Current that runs from the Philippines, along Taiwan and the Okinawan Islands to central Japan before branching off towards the central northern Pacific and Hawaii. See **Figure *4***	**YES:** High longline CPUE in the equatorial region suggest this region has the highest adult population densities.	(N Ducharme-Barth et al., 2020)
SEAPODYM	SEAPODYM predictions of yellowfin tuna larval abundance are consistent with the observations from the historic larval surveys, noting that SEAPDOYM does not fit to any data on larval distributions. Larval density is predicted by SEAPODYM based on environmental information to indicate optimal conditions for spawning and larval survival. The predictions show the highest larval densities are in the equatorial region between around 10°N to 10°S and east to about 140°W, with predicted hotspots along the north of PNG and around the Solomon Islands, and also around Philippines, south of Japan to Taiwan. SEAPODYM also predicts the increased abundance of larvae to the north of 20°N in the third and fourth quarters (summer/autumn), and south of 20°S and down the east Australian coast in the first and second quarters (summer/autumn).	**Yes:** Consistent with larval surveys, the equatorial region is the major larval habitat, with seasonal increases in larval abundance in the northern and southern regions in the respective summer/autumns in the north and southern hemisphere. Hotspots of PNG, Philippines and Taiwan. Stock replenishment would	(Lehodey et al., 2017; Nicol et al., 2022; Senina et al., 2018, 2015)

	Quarter 2 and quarter 3, are predicted to have higher larval abundance in the central Pacific, which is also consistent with the larval data. Juvenile and adults are predicted in highest abundance in the tropical western Pacific, and consistent with the CPUE patterns, although this is not surprising since SEAPODYM is fit to fishery catch data, and there is discontinuity between the areas of high abundance between the central western Pacific and the eastern Pacific, at around 140°W. See **Figure *5***	be derived mostly from the equatorial region spawning.	

b) Bigeye tuna

Information source	Summary	Support for spatial population structure in the WCPO	References
Spawning areas and larval distribution	Spawning is observed across the tropical western and central Pacific Ocean and in the seas around the Philippines and Indonesia, also southwest of Hawaii (Johnston Island area) and in the Coral Sea off northeast Australia. Spawning is also observed across a wide area in the central and eastern Pacific Ocean, although larval distributions appeared patchier in the central Pacific compared to yellowfin. Like other tropical tunas spawning typically occurs at SST > 24°and is more seasonal to the north and south of the tropics. It was noted at the SPC pre-assessment workshop that historical work by Japanese scientists on spatial patterns of bigeye spawning occurrence did not fit well with the observed larval distributions, and suggested greater levels of spawning in the central and eastern equatorial Pacific than would be expected from the patchy larval abundance data. It was further noted that larval sampling by the historic Japanese program was lower in the eastern Pacific compared to western Pacific which may explain the differences, but also that egg/larval survival might be higher in the western Pacific. While spawning appears widespread, there is evidence of larval hot spots between Philippines and Japan, in the far western Pacific region around PNG, Philippines/Indonesia, several areas in the central equatorial region, also off the central American coast in the eastern Pacific. See Figure **2**.	**Yes:** potentially separated spawning areas in the western and central Pacific, and the far eastern Pacific. Higher larval densities in the western Pacific may be related spatial variation in larval survival. The higher larval densities in the far western Pacific, northern PNG area, Indonesia/Philippines is consistent with high abundance of juvenile fish in this region, suggesting the region is likely an important source of broader stock replenishment for the WCPO. In contrast to yellowfin, bigeye spawning is not though to be common close to the main Hawaiian Islands.	(Buenafe et al., 2022; Farley et al., 2017; Ijima and Jusup, 2023; Muhling et al., 2017; Nepomuceno et al., 2020; Nikaido et al., 1991, Nishikawa et al., 1985; Reglero et al., 2014; Schaefer et al., 2005)
Small juvenile (< 40 cm FL, < 6	Young of the year bigeye tuna have been sampled from several areas of the WCPO, including; Philippines, Indonesia, Marshall Islands, Solomon Islands, Line Islands, French	**Yes:** similar to yellowfin, small juveniles are found across a broad	(Nicholas Ducharme-Barth et al., 2020; Rooker et al., 2016)

months age) nursery areas	Polynesia and around Hawaii. Similar to yellowfin, small bigeye are also commonly measured in catches from the fisheries in the archipelagic waters and seas around Indonesia/Philippines/Vietnam, and PNG/Solomon Islands, where high catches of small juveniles occur due to a combination of gears used and higher abundance.	are of the WCPO, but large numbers of small fish are caught in the Indonesia/Vietnam/ Philippines region, supports stratification of this region.	
Growth rates and maximum size	Comparisons of growth rates and maximum sizes across the Pacific suggest that bigeye in the eastern Pacific grow faster and reach larger sizes than in the western and central Pacific. The growth change across the Pacific appears to occur as a west (lower growth) to east (higher growth) cline. Considering the WCPO region itself, spatial growth variation seems subtle for the main parts of the growth curve that represent the bulk of the population and for which there is reasonable data for comparison. However, it has been suggested there are spatial differences, and fish sampled further to the east of the WCPO region reached larger sizes, consistent with the growth rate cline. However, it was cautioned that sample sizes for regional comparison were limited and unbalanced across the age range. The spatially stratified growth curves also may have been biased to different degrees due to the way otoliths were selected according to size bins. However, additional work on a larger data set of otolith weight-at-length further supported the hypothesis of faster growth in the EPO compared to the WCPO. Overall, apart from the west-east growth cline, the results are somewhat inconclusive. Similar to yellowfin, there are no/very few otolith samples for the regions north of 10°N, or south of 20°S to explore latitudinal variation.	**Yes:** appears likely that growth differences occur between the eastern and western regions of the WCPO, possibly supporting lower mixing between the western Pacific/Indonesia/Philippines region population and those in the eastern areas of the WCPO. The age-structured MFCL model cannot accommodate spatially varying growth. Length-age structured models are required to better deal with this issue.	(Aires-da-Silva et al., 2015; Farley et al., 2020, 2018, 2017; Moore et al., 2020)
Morphometrics, meristics and size at maturity	No dedicated morphometrics and meristics studies have occurred. Consistent with west-east growth variation, mean lengths at 50% maturity have been shown to increase from the western (103 cm) to central (108 cm) and eastern (135 cm) Pacific.	**Yes:** west – east cline in length at maturity.	(Farley et al., 2017)
Genetics	While genetic studies have shown differences between global ocean basins for bigeye, studies applying various techniques and more recently Single Nucleotide Polymorphisms (SNPs), have failed to provide conclusive evidence against the assumption of panmixia for bigeye in the WCPO (samples from Federated States of Micronesia, Marshall Islands, Gilbert Islands, Phoenix Islands and French Polynesia). Earlier studies at a Pacific wide scale did not find strong evidence of broad scale genetic differences across the WCPO and EPO, although sample sizes where limited, and further studies have been recommended at the Pacific wide scale. Studies comparing samples using SNPs from Indonesia with those from the Indian Ocean and Western Pacific Oceans however suggested a cline and isolation by distance between the Indian Ocean and Western Pacific Ocean through the Indonesian archipelago. In contrast comparisons of South China Sea, Philippine Sea and western	**No:** there is no evidence for genetic differentiation within the WCPO, and more broadly across the Pacific.	(Chiang et al., 2006; Grewe et al., 2019; Grewe and Hampton, 1998; Moore et al., 2020; Natasha et al., 2022; Proctor et al., 2019; Wu et al., 2014)

	Pacific Ocean using mitochondrial DNA indicate that bigeye tuna over these sampling areas constitute a single panmictic population.		
Otolith chemistry	Otolith chemistry studies have applied the same approaches for bigeye as for yellowfin, involving sampling of young-of- year from various locations in the WCPO to generate baseline 'juvenile origin' otolith chemical signatures. Then resampling the same cohorts at ages 1 and 2+ years and using the otolith core chemistry of the older fish, and the baseline signatures, to allocate the older fish to origin regions. This approach focussed on sub-adult fish from Hawaii, central equatorial (Line Islands/French Polynesia), west equatorial (Marshall Islands/Solomon Islands) and far western equatorial (Philippines/Indonesia). Thus, the conclusions are restricted to these locations, and suggested central equatorial sub-adults were derived from that area, whereas Hawaiian sub-adults were mostly derived from the central equatorial region (Line Islands, Kiribati, south of Hawaii). This is consistent with the larval distributions that show several areas of higher larval density in the central equatorial regions south, southeast and southwest of Hawaii, and the observation that spawning is not observed close to the Hawaiian main islands, but further south at Johnston Island. Studies in Indonesia found that small juvenile bigeye sampled in that area had otolith chemistry indicating they had resided in that area for their juvenile period, consistent with the results for yellowfin from the same study, and the hypothesis that this region is self-replenishing.	**Maybe:** as for yellowfin, information is not sufficient at the WCPO scale and further appropriately designed studies are required including adult life stages. There is evidence for connectivity between central equatorial spawning areas and Hawaii and support for limited movements of juveniles in the Indonesia region and Marshall Islands.	(Proctor et al., 2019; Rooker et al., 2016)
Parasites	No large-scale studies of parasites in the WCPO. Studies comparing juvenile bigeye parasites between samples from Indonesia, Maldives and Solomon Islands suggest that juvenile in these regions have not mixed, consistent with otolith chemistry that small juvenile bigeye remained in the Indonesian region as juveniles.	**Maybe:** insufficient spatial sampling throughout WCPO, but support for residency and separation of small juveniles in the Indonesia region from the broader WCPO.	(Moore et al., 2019)

Tagging	In WCPO since 1989 approximately 77,000 tagged bigeye have been released, with around 15,000 recaptures. Most releases were <100 cm FL with a mode of around 50 cm, and therefore are mostly sub-adults. Most releases have been in the tropical region between 20°N and 10°S, with highest numbers around the equatorial central-western Pacific south of Hawaii and PNG and Solomons region. There was an isolated group of tag releases in the Coral Sea adjacent to Cairns in the early 1990s, and also north of Chinese Taipei. Smaller numbers have also been released around Hawaii. Tag-recapture summaries are presented in most recent stock assessments (see **Figure 3**). Patterns of tag-recaptures show considerable movement along the equatorial region, similar to yellowfin, including movement between the WCPO and the EPO. Analysis of tag recapture patterns indicates that fish tagged in the western Pacific tend to be recaptured in that general region, and likewise for fish tagged in the central and east Pacific, but that mixing occurs between the western and central Pacific from about 180°E to the west, and between the central and eastern Pacific to the east of 150°E. This pattern supports an isolation by distance hypothesis between bigeye populations in the eastern and western Pacific. Fish tagged in the central Pacific appear to have a greater tendency to move east than west, and fish tagged in the far eastern Pacific often move west towards the central Pacific. This may support segregation of the central equatorial region. Gene flow appears high enough to maintain genetic homogeneity across the entire Pacific. The fish tagged in the Coral Sea tagging were mostly recaptured in the Coral Sea near the release area although recaptures did occur to the north and in the tropical region east of PNG/Solomons region, and some were recaptured around New Caledonia, Fiji and French Polynesia. Interestingly, very few fish tagged in the equatorial region were recapture in southern regions, south of 10°S. Releases north of Chinese Taipei tended be recaptured to the south of Japan in the Kuroshio Current area but some moved to Hawaii. Of the few recaptures of Hawaiian tagged fish some moved south to the equatorial region while others moved north and northeast as they recruited to the longline fishery (Fig 3). Studies with archival tags are consistent with those of traditional external tags. Similar to yellowfin, bigeye tagged in the Bismarck Sea and Solomons Islands area tend to show less rapid movement away from that area. Most archival tagged bigeye in the Coral Sea moved east or northeast, very few went south, one fish moved 14,580 km northeast in 874 days. See **Figure 3**.	**Yes:** similar to yellowfin, the tag-recapture data show more movement longitudinally in the equatorial region than latitudinally, supporting stratification of the tropical region. There appears to be greater residency of bigeye tagged in PNG/Solomons region, noting that the tagged fish in this area are mostly juveniles and lifetime displacement is likely underestimated, plus tag recapture rates tend to be high in this area shortly after the fish area released. There may be some support for an eastern region of the central western Pacific that is perhaps more linked to the EPO region. There appears to be more connection of equatorial tagged fish to northern than southern regions of the Pacific.	(Hampton and Gunn, 1998; Hampton and Williams, 2005; Itano and Holland, 2000; Leroy et al., 2014; Schaefer et al., 2015; Schaefer and Fuller, 2009)
CPUE spatial patterns	The longline CPUE distribution for bigeye shows a different pattern to yellowfin in that the concentration of higher CPUE is in the central and eastern Pacific, compared to yellowfin where it is in the western Pacific equatorial region. There are some isolated areas of higher	**Yes:** higher long line CPUE in the equatorial region and toward the central Pacific suggests larger	(Ducharme-Barth et al., 2020)

	CPUE in the South China Sea region, the Coral Sea (small area off Cairns, northeast Australia), north of New Zealand and east of Japan and towards Hawaii in the Kuroshio Current extension. The region of higher equatorial CPUE also extends to the north of the central equatorial region, but not to the south, which is consistent with the lack of southerly movements of bigeye tagged in the central equatorial region. Higher CPUE is also observed near Hawaii and further north, where the fishery is more seasonal. See **Figure *4***.	(adult) longline vulnerable fish are more abundant in that region than the western Pacific, where lots of smaller bigeye are caught in purse seines. Perhaps with exception of areas in the South China Sea/Philippines region.	
SEAPODYM	The predictions of larval abundance by the most recent SEAPODYM model for bigeye are somewhat consistent with those observed in the historic larval data set, in that they predict local hotspots around Indonesia/Philippines and PNG, Chinese Taipei and Okinawa Islands region. SEAPODYM however predicts three broad areas of higher larval abundance, between 20°N -30°N extending east to the north of Hawaii, equatorial from around 160°W– to the southern US and Central American coast, and a southern area, just south of the equator to around 20°S, extending from around 160°W to the Central American coast. SEAPODYM also predicts higher larval abundance along the northeast coast of Australia, extending across to Fiji and to the north of New Zealand. The historical larval data sets do not show the higher larval densities extending into the central Pacific in the northern and southern hemispheres as predicted by SEAPODYM, however, inspection of the raw larval data suggest bigeye were sampled in the northern region between Japan and Hawaii, but in very low numbers and perhaps were not predicted by the spatio-temporal models in Ijima and Jusup. SEAPODYM predictions of juveniles show high abundance in the Indonesia/Philippines/PNG archipelagic waters and seas, also in the South China Sea and off Chinese Taipei. SEAPODYM also predicts that juveniles occur in higher abundance in waters across the Pacific from about 10°N to 25°N, and from the equatorial region to around 20°S. There is a distinct hotspot prediction close to central America, off Colombia. The predictions for adult bigeye are generally similar to juveniles in being widespread across the northern and southern Pacific, but in the equatorial region being more concentrated in the central to eastern Pacific compared to the western Pacific, with the exception of some high abundance predicted in the Indonesia/Philippines/PNG archipelagic waters and seas, and in the South China Sea. See **Figure *5***	**Yes:** suggest three broad zones of larval abundance, north, equatorial and south, with the equatorial region having higher densities towards the central/eastern Pacific. Similar patterns for juveniles and adults. Support for northern, equatorial and southern strata, but that also the stock is not separated between the WCPO and the EPO.	(Senina et al., 2023, 2021, 2020)

Appendix 2 Detailed methods for the CPUE analysis using convergent cross mapping (CCM) within empirical dynamic modelling (EDM)

Datasets and CPUE standardisation

Nominal catch and effort data from Pacific Ocean pelagic longline sets made between 1950-2018 inclusive were extracted from SPC's 'L.BEST' database at 5° × 5°, monthly resolution, and aggregated to a 15° × 15° Pacific-wide grid (Figures 1, 2, 4). The dataset was filtered to remove grid cells lacking consistent time series throughout the period of interest (23 out of the 83 cells), as well as observations with extreme outlier values for the effort metric - the number of hundred hooks per set (i.e., values greater than the 99th quantile value of 5,455 hundred hooks). Our final filtered dataset contained 557,260 records.

Nominal catches for yellowfin and bigeye were standardised using single-species Tweedie generalised linear models (GLMs) with a log link fitted within the 'glmmTMB' package (Brooks et al. 2017) in R 4.1.1 (R Core Team 2021). The Tweedie distribution is a flexible three parameter distribution suitable for modelling overdispersed, non-negative continuous data, with a high density of observations at zero (Bonat and Kokonendji 2017). Models for catch in numbers (*C*) were fitted to data in each grid cell independently, and for each species included fixed effect factors for year (*Yr*), quarter (*Qtr*) and hooks per basket *(HPB)*, the latter binned into 5-hook bins, with the number of hundred hooks per set (*hhooks*) included as an effort offset term. Specifically,

$$C_{sci} \sim \mathrm{Tw}_p(\mu_{sci}, \phi)$$

$$\mu_{sci} = \exp(\eta_{sci})$$

$$\eta_{sci} = \beta_0 + \beta_x X + \mathrm{offset}(\log(hhooks_i))$$

and η_{sci} is the linear predictor for the observed species (*s*) catch, for grid cell *c*, and set *i*. Here, *x* is a vector of regression coefficients and *X* is the matrix of predictor variables. The variance of C_{sci} is assumed to be a function of the estimated dispersion ϕ and power *p* parameters (see Jorgensen 1997; Bonat and Kokonendji 2017 for further details), given by:

$$\mathrm{Var}(C_{sci}) = \phi\mu_{sci}^{p}$$

HPB backfill and modelling

The early years of the L.BEST dataset were characterised by many missing HPB values associated with otherwise reliable catch records (i.e. 61.2% missingness pre-1980; 17.8% missingness post-1980). We aimed to retain as many of these records as possible in our analysis, and so explored several methods to backfill the missing HPB values. For records between 1950 and 1980, a period when there was minimal specialised species targeting using HPB, we used historical records of flag- and area-specific HPB values, drawn from Hampton et al. (1998) (see Table 1 in that paper). From 1980 to 2018 inclusive, we fitted a series of Poisson generalised linear mixed models (GLMMs) with a log link to predict missing HPB values. These models included fixed effect factors for year (*Yr*), quarter (*Qtr*) and target species (*Targ*) (defined as the most abundant harvested species for a given set), a grid-cell level covariate for thermocline depth (*T.depth*) (drawn from the 'GODAS isotherm' database: https://psl.noaa.gov/data/gridded/data.godas.html), a random intercept for a combination flag/fleet variable (*FF*) variable and a spatial random effect (ω). We began with the full model, comprising all fixed and random effects, and used a top-down, AIC-based approach to arrive at the best supported random and fixed effects structures (see Zuur et al. 2009). The final model was of the form:

$$HPB_{ijk} \sim \text{Poisson}(\mu_{ijk})$$

$$\log(\mu_{ijk}) = \eta_{ijk}$$

$$\eta_{ijk} = \beta_0 + \beta_1 Yr_{ijk} + \beta_2 Qtr_{ijk} + \beta_3 Targ_{ijk} + a_j^{FF} + b_k^{\omega}$$

$$a_j^{FF} \sim \text{N}(0, \sigma_{FF}^2)$$

$$b_k^{\omega} \sim \text{N}(0, \sigma_{\omega}^2)$$

where HPB_{ijk}, the observed HPB for set *i*, flag/fleet *j* and spatial knot *k*, is Poisson distributed with mean μ_{ijk}, and η_{ijk} is the linear predictor. The a_j^{FF} and b_k^{ω} terms allow for different intercepts for each flag/fleet and spatial knot, and are assumed to be normally distributed with mean 0 and variance σ_{FF}^2 and σ_{ω}^2, respectively. We tested for overdispersion by computing an estimate of the dispersion parameter, given by the square root of the penalised residual sum of squares divided by the number of observations. This was equal to ~1.25 and was deemed small enough to stay with the Poisson model for the purposes of our analysis. Plots of quantile residuals generated from the 'DHARMa' package (Hartig 2022) indicated an adequate fit to the data. The model provided reasonable predictive performance (Pearson correlation of 0.82 between observed and predicted HPB values), though there was a tendency to overpredict small HPB values. For records in our dataset where observed HPB was missing, we used the predicted HPB from this model as the final HPB for use in CPUE standardisation.

Empirical dynamic modelling

Empirical dynamic modelling (EDM) is a non-linear statistical approach that can be used to reconstruct the dynamics of a system directly from time series data and to make forecasts about that system (Takens 1981; Deyle and Sugihara 2011). The method assumes nothing about the equations controlling a system's dynamics. Convergent cross mapping (CCM) uses the mathematical theory of EDM to uncover causal relationships between time series variables, allowing statements to be made on if these variables belong to the same dynamical system (see Sugihara et al. 2012; Chang et al. 2017; Munch et al. 2018, 2020).

Given previous successes in applying non-linear time series analysis and multivariate state-space reconstruction to fisheries data (e.g. Glaser et al. 2011, 2014; Deyle et al. 2013), we considered that the CCM approach may prove useful for understanding if the dynamics driving longline CPUE trends for yellowfin and bigeye are similar across the Pacific, and if so, at what spatial scale are these trends related and predictable. Visualising the CCM results using a clustering approach could then provide an objective means for defining candidate spatial structures for the 2023 assessments that capture both the human and ecological components of the longline fishery system.

Simulations

First, we used simulations to test the utility of the method under controlled settings. Working with the same 15° × 15° Pacific-wide grid described earlier (see Figure 1), we simulated CPUE time series for each cell from a spatially explicit population dynamics model with flexibility to vary diffusion, fishing intensity, recruitment and environmental effects (i.e. sea surface temperature) on recruitment and survival.

We explored 18 simulation scenarios designed to emulate realistic patterns in CPUE trends for fish populations exhibiting simple to complex spatio-temporal dynamics, using time series comprising 60 (scenarios 'real1'-'real6'), 100 (scenarios 'basic1'-'basic6') or 1000 (scenarios 'full1'-'full6') time steps. For each scenario, we generated 10 additional 'white noise' time series (r1-r10), each a sequence of iid random variables with mean ≈ 0, SD ≈ 1 of length equal to the number of time steps considered for that scenario. The white noise time series were inherently unpredictable, and were used to gauge the sensitivity of the method to distinguish random from predictable time series.

For each scenario, we then applied CCM using a set of customised functions modified from the 'rEDM' package (Ye et al. 2019) to estimate the predictability between time series pairs. The CCM output is a Euclidean distance matrix relating each time series pair. Next, we applied a fuzzy (probabilistic) clustering approach on the resulting matrix in the 'cluster' package (Maechler et al. 2022) to identify and visualise the spatial patterns in time series (and hence the grid cells) that share dynamics across the region. We used the simulation scenarios to explore the sensitivity of the cluster outputs to different values of the *memb.exp* arguments in the 'fanny' function. This argument controls the relative crispness of the clustering and can have a strong impact on the robustness of fuzzy clustering algorithms (Wu 2012). We found that setting *memb.exp* = 1.2 provided the best balance between crispness and fuzziness across all simulation scenarios, and so kept this same value for the yellowfin and bigeye CPUE analyses.

Key results from the simulations

In general, the CCM accurately recovered the spatial structures we simulated. For example, Figure 1 shows results for scenario 'basic3', one characterised by moderate spatio-temporal complexity in dynamics and moderate time series length. The CCM correctly identified the four spatial divisions we set up in the simulation, with crisp delineation evident among clusters and each cell assigned to its cluster with high probability. The CCM also accurately differentiated the white noise time series r1-r10 (shown as light blue circles), which were all classified as a separate cluster with no overlap with any cells containing simulated CPUE series.

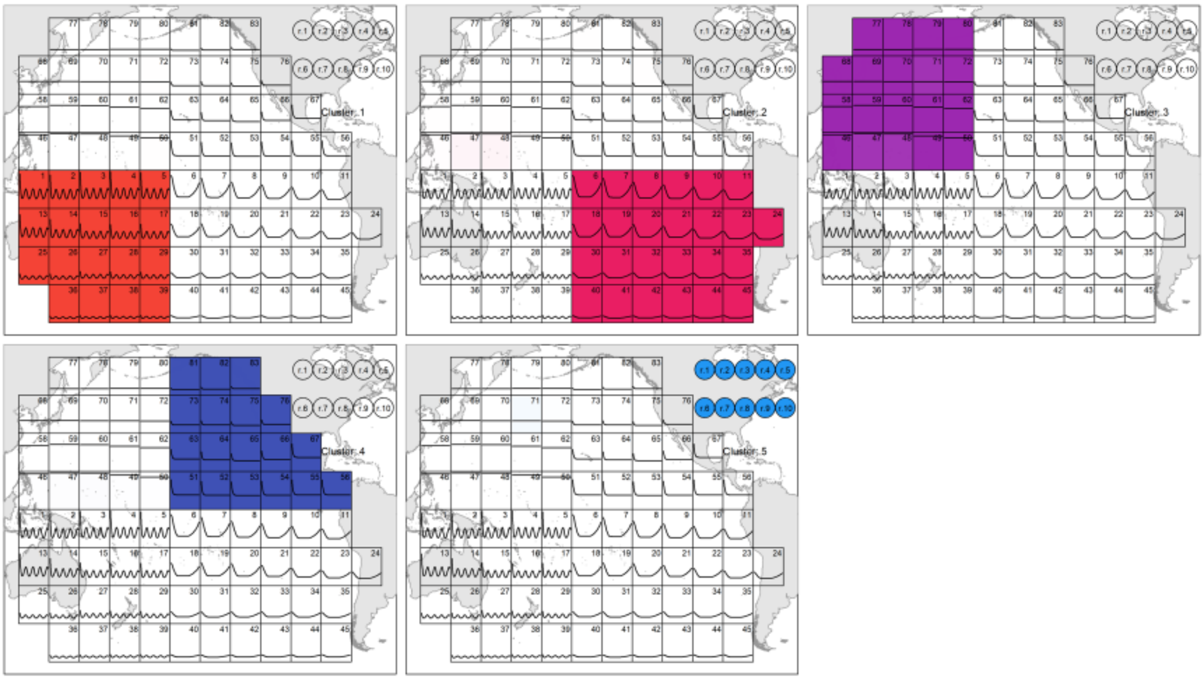

Figure 1. Results from the CCM/fuzzy clustering approach applied on simulation scenario 'basic3'. Black lines in each 15° × 15° grid cell represent simulated CPUE trends drawn from the spatial population dynamics model plotted across 100 time steps. The circles at the top right corner of each panel reflect white noise process time series that are in essence unpredictable. The different colours in the plot signify different clusters and the shade of the colour for each grid cell reflects the probability of that cell falling within a particular cluster. Darker colours reflect higher probabilities, more transparency reflecting lower probabilities. Grid cells ids are numeric references for the CCM/clustering approach.

Comparable results were observed across the other simulation scenarios. Clusters were typically clearly defined and characterised by arrangements of contiguous cells with high assignment probabilities of cells to clusters. We did find that both the smoothness and the length of the time series influenced our capacity to recover the spatial patterns generated in the simulations. Yet overall, this simulation exercise demonstrated that CCM can accurately delineate known spatial structure in time series exhibiting a range of dynamics, and that combining CCM predictions with fuzzy clustering provides a useful tool for visualising CCM outputs across a large spatial domain.